NASA Contractor Report 4152

Acousto-Ultrasonic Input-Output Characterization of Unidirectional Fiber Composite Plate by SV Waves

Peter Liao and James H. Williams, Jr.

GRANT NAG3-328
JUNE 1988

NASA

NASA Contractor Report 4152

Acousto-Ultrasonic Input-Output Characterization of Unidirectional Fiber Composite Plate by SV Waves

Peter Liao and James H. Williams, Jr.
Massachusetts Institute of Technology
Cambridge, Massachusetts

Prepared for
Lewis Research Center
under Grant NAG3-328

National Aeronautics
and Space Administration

**Scientific and Technical
Information Division**

1988

ABSTRACT

A unidirectional fiberglass epoxy composite specimen is modelled as a homogeneous transversely isotropic continuum plate medium. Acousto-ultrasonic non-contact input-output characterization by tracing SV waves in the continuum is studied theoretically with a transmitting and a receiving transducer located on the same face of the plate. The isotropic plane of the equivalent continuum plate model lies in the midplane of the plate and is parallel to the top and bottom faces of the plate.

The single reflection problem for an incident SV wave at a stress-free plane boundary in a semi-infinite transversely isotropic medium whose isotropic plane is parallel to the plane boundary is analyzed first. For all angles of incidence, the angle of reflection of the SV wave is equal to the angle of incidence of the SV wave. It is found that an obliquely incident SV wave results in a reflected SV wave and a reflected P wave for an angle of incidence of the incident SV wave less than the critical angle 52°. when the angle of incidence of an incident SV wave is equal to or greater than the critical angle, there exists only an SV wave in the medium as the reflected P wave degenerates into a surface wave travelling parallel to the plane boundary. The amplitude of the surface wave decays exponentially with the perpendicular distance from the plane boundary. The amplitude

ratios of the reflected P and SV waves to the incident SV wave as a function of the angle of incidence are plotted from zero to the critical angle. The amplitude ratio of the reflected SV wave is found to be minus one when the angle of incidence is equal to or greater than the critical angle. The balance in energy flux normal to the plane boundary is checked.

Accordingly, the delay time for wave propagation between the transmitting and the receiving transducers is computed as if the SV waves were propagating in a half space. It is found that the directional dependence of the phase velocity of the SV wave propagating in the transversely isotropic medium has a significant effect on the delay time, as opposed to the directional independence of the phase velocity of a shear wave propagating in an isotropic medium.

The displacements associated with the SV wave in the plate and which may be detected by the non-contact receiving transducer are approximated by an asymptotic solution for an infinite transversely isotropic medium subjected to a harmonic point load. The polar diagrams for the directivity function of the stresses due to SV waves in the plate are shown at frequencies of 0.75, 1.50 and 2.25 MHz.

This study enhances the quantitative understanding of acousto-ultrasonic non-destructive evaluation (NDE) parameters such as the stress wave factor (SWF) and wave propagation in fiber reinforced polymeric, ceramic or metallic composites, which can be modelled as transversely isotropic media.

INTRODUCTION

Fiber reinforced composite materials are attractive materials for aerospace applications because of their high specific mechanical properties. It has been shown that many composites, such as fiberglass epoxy composites or fiber reinforced ceramics as shown in Fig. 1, may be modelled as a homogeneous transversely isotropic continuum [1]. In this work, acousto-ultrasonic (AU) non-contact input-output characterization of a homogeneous transversely isotropic elastic plate is investigated by tracing SV waves.

First, the single reflection problem of an incident SV wave at a stress-free plane boundary in a semi-infinite transversely isotropic medium whose isotropic plane is parallel to the plane boundary is considered. At such boundaries, the conditions for the existence of wave mode conversion, critical angle phenomena, reflected surface wave, the angles of reflection of the reflected waves, and the amplitude ratios of the reflected waves to the incident wave are derived.

Second, the SV wave input-output relations are derived when multiple reflections occur at the top and the bottom faces of the plate. The delay time between input and output versus the dis-

tance separating the transmitting and receiving transducers is analyzed. The directivity functions of the stresses associated with the SV waves are computed. And, the output displacement at the non-contact receiving transducer is approximated by an asymptotic solution.

This investigation should enhance the quantitative understanding of AU NDE parameters such as the stress wave factor. It also provides the potential for assisting in the development of better NDE schemes utilizing the SWF as well as other AU parameters for the characterization of fiber reinforced polymeric, metal and ceramic composites.

SINGLE REFLECTION PROBLEM AT STRESS-FREE PLANE BOUNDARY IN SEMI-INFINITE TRANSVERSELY ISOTROPIC MEDIUM WHOSE ISOTROPIC PLANE IS PARALLEL TO PLANE BOUNDARY FOR INCIDENT SV WAVE

1. Reflected P and SV Waves

For a homogeneous linearly elastic transversely isotropic continuum, the number of independent elastic constants is five [1]. Define a coordinate system (x, y, z) for a semi-infinite transversely isotropic medium whose isotropic plane is parallel to the plane boundary where the reflection occurs as follows: the plane boundary contains the x and y axes, and the z axis is the zonal axis of the medium, which is in the direction parallel to the fiber direction shown in Fig. 1. Also, see Fig. 2. The generalized Hooke's law is written, relative to the (x, y, z) coordinate system, as [1]

$$
\begin{aligned}
\tau_{xx} &= C_{11}u,x + C_{12}v,y + C_{13}w,z \\
\tau_{yy} &= C_{12}u,x + C_{11}v,y + C_{13}w,z \\
\tau_{zz} &= C_{13}u,x + C_{13}v,y + C_{33}w,z \\
\tau_{xz} &= C_{44}(u,z + w,x) \\
\tau_{yz} &= C_{44}(v,z + w,y) \\
\tau_{xy} &= C_{66}(u,y + v,x)
\end{aligned}
\tag{1}
$$

where τ_{rs} (r, s = x, y and z) are the normal (r = s) and shear

($r \neq s$) stresses with respect to the coordinate system (x, y, z); u, v and w are the displacement components of a point in the medium along the x, y and z axes, respectively; "," denotes partial differentiation with respect to the variable which follows; and C_{11}, C_{12}, C_{13}, C_{33} and C_{44} are the five independent elastic constants where $C_{66} = 1/2(C_{11} - C_{12})$.

Let a progressive wave be represented as [2]

$$(u, v, w) = A\,(P_x, P_y, P_z)\,\exp\{i\omega(S_x x + S_y y + S_z z - t)\} \qquad (2)$$

where S_x, S_y and S_z are the components of the slowness vector, which is in the same direction as the normal to the wavefront and whose magnitude is equal to the reciprocal of the magnitude of the phase velocity [1], along the x, y and z axes, respectively; P_x, P_y and P_z are the components of a unit vector of particle displacement along the x, y and z axes, respectively; A is the amplitude of particle displacement; t denotes time and ω denotes radian frequency. It follows from Eqs. (1) and (2) that the stresses can be represented as

$$\tau_{xx} = i\omega A[C_{11}S_xP_x + C_{12}S_yP_y + C_{13}S_zP_z]\exp\{i\omega(S_x x + S_y y + S_z z - t)\}$$

$$\tau_{yy} = i\omega A[C_{12}S_xP_x + C_{11}S_yP_y + C_{13}S_zP_z]\exp\{i\omega(S_x x + S_y y + S_z z - t)\}$$

$$\tau_{zz} = i\omega A[C_{13}S_xP_x + C_{13}S_yP_y + C_{33}S_zP_z]\exp\{i\omega(S_x x + S_y y + S_z z - t)\}$$

$$\tau_{xz} = i\omega A[C_{44}S_zP_x + C_{44}S_xP_z]\exp\{i\omega(S_xx + S_yy + S_zz - t)\} \quad (3)$$

$$\tau_{yz} = i\omega A[C_{44}S_zP_y + C_{44}S_yP_z]\exp\{i\omega(S_xx + S_yy + S_zz - t)\}$$

$$\tau_{xy} = i\omega A[C_{66}S_yP_x + C_{66}S_xP_y]\exp\{i\omega(S_xx + S_yy + S_zz - t)\}$$

The stress boundary conditions on the stress-free plane boundary require that [2]

$$\begin{aligned} \tau_{xz}^{(I)} + \tau_{xz}^{(R)} &= 0 \\ \tau_{yz}^{(I)} + \tau_{yz}^{(R)} &= 0 \\ \tau_{zz}^{(I)} + \tau_{zz}^{(R)} &= 0 \end{aligned} \quad (4)$$

where $\tau_{rz}^{(I)}$ (r = x, y and z) represent stresses on the plane boundary associated with the incident SV wave, and $\tau_{rz}^{(R)}$ (r = x, y and z) represent stresses on the plane boundary associated with the reflected waves.

In order to satisfy Eq. (4), it is required [2] that the frequency, ω, of the reflected wave be equal to that of the incident wave and that [2]

$$\begin{aligned} S_x^{(I)} &= S_x^{(R)} \\ S_y^{(I)} &= S_y^{(R)} \end{aligned} \quad (5)$$

As a result of Eq. (5), the slowness vectors of the incident and reflected waves lie in a plane called the plane of incidence. This analysis can be simplified by assuming that the plane of incidence is the $x = 0$ plane; that is, the slowness vectors of the incident and reflected waves are in the $x = 0$ plane, as shown in Fig. 2. Then it follows from Eqs. (5) that

$$S_x^{(I)} = S_x^{(R)} = 0 \tag{6}$$

It has been shown [3] that, except along the principal material axes, P waves or SV waves travelling in a plane containing the zonal axis, z axis, of a transversely isotropic medium are quasi-longitudinal and quasi-transverse, respectively; that is, in general, the components of the unit vector of particle displacement for either the P or SV waves along the y and z axes, P_y and P_z, do not vanish; whereas the components along the x axis, P_x, do vanish. Therefore, it follows from Eqs. (3) and (6) that stresses associated with P and SV waves are

$$\begin{gathered} \tau_{xz} = \tau_{xy} = 0 \\ \tau_{xx} \neq 0;\ \tau_{yy} \neq 0;\ \tau_{zz} \neq 0;\ \tau_{yz} \neq 0 \end{gathered} \tag{7}$$

It has also been shown that an SH wave travelling in a plane containing the zonal axis,z axis, of a transversely isotropic

medium possesses a transverse displacement only, that is, for the coordinates in Fig. 2, $(P_x, P_y, P_z) = (1, 0, 0)$ [3]. Therefore, it follows from Eqs. (3) and (6) that the stresses associated with SH waves are

$$\begin{gathered} \tau_{yz} = \tau_{xx} = \tau_{yy} = \tau_{zz} = 0 \\ \tau_{xy} \neq 0; \ \tau_{xz} \neq 0 \end{gathered} \tag{8}$$

Assume that an SV wave is incident on the plane boundary, the x-y plane in Fig. 2. It follows from Eqs. (4) and (7) that

$$\begin{gathered} \tau_{yz}^{(I)} \neq 0 \ ; \quad \tau_{zz}^{(I)} \neq 0 \\ \tau_{xz}^{(I)} = 0 \end{gathered} \tag{9}$$

As a result of Eq. (9), it is known from Eq. (4) that $\tau_{xz}^{(R)}$ is equal to zero. This means that no SH wave will be reflected back into the medium because a reflected wave of the SH type would result in a nonzero value of the stress τ_{xz}. So, Eqs. (4) reduce to

$$\begin{aligned} \tau_{yz}^{(I)} + \tau_{yz}^{(R)} &= 0 \\ \tau_{zz}^{(I)} + \tau_{zz}^{(R)} &= 0 \end{aligned} \tag{10}$$

Since either a reflected P wave or a reflected SV wave results in nonzero values of the stresses $\tau_{yz}^{(R)}$ and $\tau_{zz}^{(R)}$, it is therefore concluded from Eqs. (7) and (10) that both a P wave and an SV wave may be reflected back into the medium.

2. Slowness Surface for P and SV Waves

The equations of motion relative to the coordinate system (x, y, z) are [1]

$$\begin{aligned} \tau_{xx,x} + \tau_{xy,y} + \tau_{xz,z} &= \rho u,tt \\ \tau_{xy,x} + \tau_{yy,y} + \tau_{yz,z} &= \rho v,tt \\ \tau_{xz,x} + \tau_{yz,y} + \tau_{zz,z} &= \rho w,tt \end{aligned} \tag{11}$$

where the body forces are identically zero for the homogeneous solution.

It follows from Eqs. (1), (2) and (11) that the following equations of motion are obtained:

$$\begin{aligned} &[C_{11}S_x^2 + C_{66}S_y^2 + C_{44}S_z^2 - \rho]P_x + (C_{12} + C_{66})S_xS_yP_y \\ &\qquad + (C_{13} + C_{44})S_xS_zP_z = 0 \end{aligned}$$

$$(C_{12} + C_{66})S_xS_yP_x + [C_{66}S_x^2 + C_{11}S_y^2 + C_{44}S_z^2 - \rho]P_y + (C_{13} + C_{44})S_yS_zP_z = 0 \qquad (12)$$

$$(C_{13} + C_{44})S_xS_zP_x + (C_{13} + C_{44})S_yS_zP_y + [C_{44}(S_x^2 + S_y^2) + C_{33}S_z^2 - \rho]P_z = 0$$

The condition for the existence of the plane wave solution is expressed by setting the determinant of the matrix of the coefficients of P_x, P_y and P_z in Eq. (12) equal to zero [1]:

$$\begin{vmatrix} [C_{11}S_x^2 + C_{66}S_y^2 + C_{44}S_z^2 - \rho] & (C_{12} + C_{66})S_xS_y & (C_{13} + C_{44})S_xS_z \\ (C_{12} + C_{66})S_xS_y & [C_{66}S_x^2 + C_{11}S_y^2 + C_{44}S_z^2 - \rho] & (C_{13} + C_{44})S_yS_z \\ (C_{13} + C_{44})S_xS_z & (C_{13} + C_{44})S_yS_z & [C_{44}(S_x^2 + S_y^2) + C_{33}S_z^2 - \rho] \end{vmatrix} = 0 \qquad (13)$$

By expanding Eq. (13), three sheets of slowness surface are obtained. The slowness surface for an SV wave is given in [3] as

$$\left(\frac{C_{11} + C_{44}}{2}\right)(S_x^2 + S_y^2) + \left(\frac{C_{44} + C_{33}}{2}\right)S_z^2 - 1/2\left\{\left[(C_{11} - C_{44})(S_x^2 + S_y^2) + (C_{33} - C_{44})S_z^2\right]^2 + 4(S_x^2 + S_y^2)S_z^2\left[(C_{11} - C_{44})(C_{33} - C_{44}) - (C_{13} + C_{44})^2\right]\right\}^{1/2} = \rho \qquad (14)$$

where S_x, S_y and S_z are the components of the slowness vector for an SV wave along the x, y and z axes, respectively; ρ is density; and C_{11}, C_{13}, C_{33} and C_{44} are elastic constants. Similarly, the slowness surface for a P wave is [3]

$$\left(\frac{C_{11} + C_{44}}{2}\right)(S_x^2 + S_y^2) + \left(\frac{C_{33} + C_{44}}{2}\right)S_z^2 + 1/2\left\{\left[(C_{11} - C_{44})(S_x^2 + S_y^2) + (C_{33} - C_{44})S_z^2\right]^2 + 4(S_x^2 + S_y^2)S_z^2\left[(C_{11} - C_{44})(C_{33} + C_{44}) - (C_{13} + C_{44})^2\right]\right\}^{1/2} = \rho \qquad (15)$$

where S_x, S_y and S_z are the components of the slowness vector for a P wave along the x, y and z axes, respectively.

One quadrant of the intersection of the slowness surface of an SV wave in the unidirectional fiberglass epoxy composite shown in Fig. 1 with the plane x = 0 and one quadrant of the intersection of the slowness surface of a P wave in the unidirectional fiberglass epoxy composite with the plane x = 0 are shown from Eqs. (14) and (15) in Fig. 3; where the numerical values of the elastic constants and density given in [1] for the unidirectional fiberglass epoxy composite are used and are as follow: C_{11} = 10.581 x $10^9 N/m^2$, C_{13} = 4.679 x $10^9 N/m^2$, C_{33} = 40.741 x $10^9 N/m^2$, C_{44} = 4.422 x $10^9 N/m^2$, and ρ = 1850 kg/m^3.

3. Angle of Reflection

It follows from Eqs. (5) and (6) that the y-component of the slowness vector of an incident SV wave is equal to the y-component of the reflected SV wave as well as the y-component of the reflected P wave. Accordingly, the relation between the y-component of the slowness vector of an incident SV wave and the y-component of the slowness vectors of the reflected SV and P waves is given as

$$S_y^{(I)} = S_y^{(SV)} = S_y^{(P)} = b \tag{16}$$

where $S_y^{(I)}$ represents the y-component of the slowness vector of an incident SV wave; $S_y^{(SV)}$ represents the y-component of the slowness vector of the reflected SV wave; $S_y^{(P)}$ represents the y-component of the slowness vector of the reflected P wave; and b is a common constant, as shown in Fig. 3.

It follows from Eqs. (6), (14) and (16) that the relation between the z-component of the slowness vector of an incident SV wave and that of the reflected SV wave is

$$S_z^{(I)} = - S_z^{(SV)} \tag{17}$$

The minus sign is due to the fact that the slowness vector of an

incident SV wave points out of the medium, whereas the slowness vector of the reflected SV wave points into the medium, as shown in Fig. 2. Consequently, the value of the z-component of the slowness vector of an incident SV wave, $S_z^{(I)}$, is negative, whereas that of the reflected SV wave, $S_z^{(SV)}$, is positive.

The angle of reflection is defined as the angle between the slowness vector of a reflected wave, either type P or SV, and the normal to the plane boundary where the reflection occurs. Similarly, the angle of incidence is defined as the angle between the slowness vector of an incident SV wave and the normal to the plane boundary, as shown in Fig. 2. Therefore, the angle of reflection of a reflected SV wave θ_{SV} is defined as

$$\theta_{SV} = \tan^{-1}(S_y^{(SV)}/S_z^{(SV)}) \tag{18}$$

and the angle of incidence of an incident SV wave θ_I is defined as

$$\theta_I = \tan^{-1}(S_y^{(I)}/-S_z^{(I)}) \tag{19}$$

It follows from Eqs. (16) through (19) that, for all angles, the angle of incidence of an incident SV wave is equal to the angle of reflection of the reflected SV wave, as shown in Fig. 2.

However, the angle of reflection of the reflected P wave is not equal to the angle of incidence of the incident SV wave. For a given value of b in Eq. (16), two values of the z-component of the slowness vector, S_z, of equal magnitude but opposite sign (for a P wave travelling in the plane $x = 0$ in the transversely isotropic medium) can be obtained from the slowness surface for the P wave by substituting Eqs. (6) and (16) into Eq. (15). The positive z-component of the slowness vector corresponds to the reflected P wave and is denoted as $S_z^{(P)}$. Similarly, for a given value of b, there exists a positive z-component of the slowness vector, $S_z^{(SV)}$, corresponding to the reflected SV wave. Accordingly, for any given value of b in Eq. (16), there exist a positive z-component of the slowness vector for the reflected SV wave, $S_z^{(SV)}$, and a positive z-component of the slowness vector for the reflected P wave, $S_z^{(P)}$. In fact, the z-components of the slowness vectors of the reflected SV and P waves, $S_z^{(SV)}$ and $S_z^{(P)}$, for an incident SV wave which determines the value of b in Eq. (16) and which travels in the plane $x = 0$ in the transversely isotropic continuum, can be obtained from the lengths of the perpendicular lines between the abscissa representing the value of b and the intersections with the two sheets of the slowness surfaces for the reflected SV and the reflected P waves, respectively, as shown in Fig. 3. It is apparent from Fig. 3 that the z-component of the slowness vector of the reflected SV wave,

$S_z^{(SV)}$, is greater than that of the reflected P wave, $S_z^{(P)}$, for an incident SV wave travelling in the plane x = 0 in the unidirectional fiberglass epoxy composite [1]. Consequently, the angle of reflection of the reflected P wave θ_p, defined similarly to Eq. (18) as

$$\theta_p = \tan^{-1}(S_y^{(P)}/S_z^{(P)}), \tag{20}$$

is larger than the angle of reflection of the reflected SV wave for an incident SV wave in the unidirectional fiberglass epoxy composite, from Eqs. (16), (18) and (20).

The critical angle is defined as the angle of incidence of an incident SV wave at which the slowness vector of the reflected P wave becomes tangent to the plane boundary where the reflection occurs. For the specific case of an incident SV wave in the unidirectional fiberglass epoxy composite in Fig. 1, it has been shown above that the angle of reflection of the reflected P wave is greater than that of the reflected SV wave. Thus, the critical angle phenomenon occurs for this composite. The critical angle for an incident SV wave in the unidirectional fiberglass epoxy composite shown in Fig. 1 is equal to 52°. The angle of reflection of the reflected P wave versus the angle of incidence of an incident SV wave in the unidirectional fiberglass epoxy

composite [1] is plotted from zero to the critical angle 52°, as shown in Fig. 4.

4. Amplitude Ratios of Reflected Waves to Incident Wave for Angle of Incidence Less Than Critical Angle

It has been stated that an SV wave and a P wave will be reflected back into the semi-infinite transversely isotropic medium if the angle of incidence of the SV wave incident on the plane boundary is less than the critical angle. The stress boundary conditions for an incident SV wave whose slowness vector is in the plane $x = 0$ can be rewritten, from Eqs. (4) and (7), as

$$\begin{aligned} \tau_{yz}^{(I)} + \tau_{yz}^{(SV)} + \tau_{yz}^{(P)} &= 0 \\ \tau_{zz}^{(I)} + \tau_{zz}^{(SV)} + \tau_{zz}^{(P)} &= 0 \end{aligned} \tag{21}$$

where $\tau_{yz}^{(I)}$ and $\tau_{zz}^{(I)}$ represent the shear and normal stresses associated with the incident SV wave; $\tau_{yz}^{(SV)}$ and $\tau_{zz}^{(SV)}$ represent the shear and normal stresses associated with the reflected SV wave; and $\tau_{yz}^{(P)}$ and $\tau_{zz}^{(P)}$ represent the shear and the normal stresses associated with the reflected P wave.

The shear stress, $\tau_{yz}^{(I)}$, associated with an SV wave of unit amplitude travelling in the plane $x = 0$ and incident on the plane

boundary at the origin, as shown in Fig. 2, can be obtained from Eqs. (3) and (6) as

$$\tau_{yz}^{(I)} = i\omega(C_{55}S_z^{(I)}P_y^{(I)} + C_{55}S_y^{(I)}P_z^{(I)}) \tag{22}$$

where $P_y^{(I)}$ and $P_z^{(I)}$ are the components of the unit vector of particle displacement of the incident SV wave along the y and z axes, respectively. Similarly, the normal stress, $\tau_{zz}^{(I)}$, associated with the incident SV wave of unit amplitude can be expressed, from Eqs. (3) and (6) as

$$\tau_{zz}^{(I)} = i\omega(C_{13}S_y^{(I)}P_y^{(I)} + C_{33}S_z^{(I)}P_z^{(I)}) \tag{23}$$

The shear stress, $\tau_{yz}^{(SV)}$, and the normal stress, $\tau_{zz}^{(SV)}$, associated with the reflected SV wave on the plane boundary at the origin are, from Eqs. (3) and (6)

$$\tau_{yz}^{(SV)} = i\omega A^{(SV)}(C_{55}S_z^{(SV)}P_y^{(SV)} + C_{55}S_y^{(SV)}P_z^{(SV)}) \tag{24}$$

and

$$\tau_{zz}^{(SV)} = i\omega A^{(SV)}(C_{13}S_y^{(SV)}P_y^{(SV)} + C_{33}S_z^{(SV)}P_z^{(SV)}) \tag{25}$$

where $P_y^{(SV)}$ and $P_z^{(SV)}$ are the components of the unit vector of particle displacement of the reflected SV wave along the y and z

axes, respectively; and $A^{(SV)}$ is the amplitude of the reflected SV wave.

The shear stress, $\tau_{yz}^{(P)}$, and the normal stress, $\tau_{zz}^{(P)}$, associated with the reflected P wave on the plane boundary at the origin are, from Eqs. (3) and (6),

$$\tau_{yz}^{(P)} = i\omega A^{(P)}(C_{55}S_z^{(P)}P_y^{(P)} + C_{55}S_y^{(P)}P_z^{(P)}) \tag{26}$$

and

$$\tau_{zz}^{(P)} = i\omega A^{(P)}(C_{13}S_y^{(P)}P_y^{(P)} + C_{33}S_z^{(P)}P_z^{(P)}) \tag{27}$$

where $P_y^{(P)}$ and $P_z^{(P)}$ are the components of the unit vector of particle displacement of the reflected P wave along the y and z axes, respectively; and $A^{(P)}$ is the amplitude of the reflected P wave.

Upon substitution of Eqs. (22) through (27) into Eq. (21), the stress boundary conditions for an incident SV wave of unit amplitude travelling in the plane $x = 0$ can be expressed as

$$S_z^{(I)}P_y^{(I)} + S_y^{(I)}P_z^{(I)} + A^{(P)}(S_z^{(P)}P_y^{(P)} + S_y^{(P)}P_z^{(P)}) + A^{(SV)}(S_z^{(SV)}P_y^{(SV)} + S_y^{(SV)}P_z^{(SV)}) = 0 \tag{28}$$

$$(C_{13}S_y^{(I)}P_y^{(I)} + C_{33}S_z^{(I)}P_z^{(I)}) + A^{(P)}(C_{13}S_y^{(P)}P_y^{(P)} + C_{33}S_z^{(P)}P_z^{(P)}) + A^{(SV)}(C_{13}S_y^{(SV)}P_y^{(SV)} + C_{33}S_z^{(SV)}P_z^{(SV)}) = 0$$

The components of a unit vector of particle displacement along the y and z axes of an SV wave travelling in any plane containing the zonal axis of a transversely isotropic medium are given in [3], and when applied to the present case of the reflected SV wave travelling in the plane $x = 0$, can be expressed as

$$P_y^{(SV)} = \left[H_{SV} - (C_{33} - C_{44})S_z^{(SV)2}\right] \Big/ \left\{\left[H_{SV} - (C_{33} - C_{44})S_z^{(SV)2}\right]^2 + \left[(C_{13} + C_{44})S_y^{(SV)}S_z^{(SV)}\right]^2\right\}^{1/2} \tag{29}$$

$$P_z^{(SV)} = \left[(C_{13} + C_{44})S_y^{(SV)}S_z^{(SV)}\right] \Big/ \left\{\left[H_{SV} - (C_{33} - C_{44})S_z^{(SV)2}\right]^2 + \left[(C_{13} + C_{44})S_y^{(SV)}S_z^{(SV)}\right]^2\right\}^{1/2}$$

where H_{SV} is defined as

$$H_{SV} = \Big\{(C_{11} - C_{44})S_y(SV)^2 + (C_{33} - C_{44})S_y(SV)^2 - \Big\{\Big[(C_{11} - C_{44})S_y(SV)^2 + (C_{33} - C_{44})S_z(SV)^2\Big]^2 - 4S_y(SV)^2 S_z(SV)^2\Big[(C_{11} - C_{44})(C_{33} - C_{44}) - (C_{13} + C_{44})^2\Big]^2\Big\}^{1/2}\Big\} \Big/ 2$$

Similarly, the components of a unit vector of particle displacement along the y and z axes for the reflected P wave travelling in the plane x = 0 can be expressed as

$$P_y(P) = \Big[H_P - (C_{33} - C_{44})S_z(P)^2\Big] \Big/ \Big\{\Big[H_P - (C_{33} - C_{44})S_z(P)^2\Big]^2 + \Big[(C_{13} + C_{44})S_y(P)S_z(P)\Big]^2\Big\}^{1/2} \tag{30}$$

$$P_z(P) = \Big[(C_{13} + C_{44})S_y(P)S_z(P)\Big] \Big/ \Big\{\Big[H_P - (C_{33} - C_{44})S_z(P)^2\Big]^2 + \Big[(C_{13} + C_{44})S_y(P)S_z(P)\Big]^2\Big\}^{1/2}$$

where H_P is defined as

$$H_P = \Big\{(C_{11} - C_{44})S_y^{(P)2} + (C_{33} - C_{44})S_z^{(P)2} + \Big\{\Big[(C_{11} - C_{44})S_y^{(P)2} + (C_{33} - C_{44})S_z^{(P)2}\Big]^2 - 4S_y^{(P)2}S_z^{(P)2}\Big[(C_{11} - C_{44})(C_{33} - C_{44}) - (C_{13} + C_{44})^2\Big]^2\Big\}^{1/2}\Big\} \Big/ 2$$

The amplitude ratios of the reflected SV and P waves, $A^{(SV)}$ and $A^{(P)}$, for an incident SV wave of unit amplitude whose angle of incidence is less than the critical angle can be determined from Eq. (28). For a given incident SV wave, the values of the components of the slowness vector along the y and z axes, $S_y^{(I)}$ and $S_z^{(I)}$, and the values of the components of the unit vector of particle displacement along the y and z axes, $P_y^{(I)}$ and $P_z^{(I)}$, are defined as part of the specification of the incident SV wave. The values of the components of the slowness vector of the reflected SV wave along the y and z axes, $S_y^{(SV)}$ and $S_z^{(SV)}$, are determined from Eq. (16) and (17), respectively. The values of the components of the unit vector of particle displacement along the y and z axes for the reflected SV wave, $P_y^{(SV)}$ and $P_z^{(SV)}$,

are obtained by substituting $S_y^{(SV)}$ and $S_z^{(SV)}$ into Eq. (29). The values of the coefficients for $A^{(SV)}$ in Eq. (28) are thus obtained. Since the y-component of the slowness vector of the reflected P wave, $S_y^{(P)}$, is equal to that of the incident SV wave, Eq. (16), the value of the z-component of the reflected P wave, $S_z^{(P)}$, is obtained by substituting $S_y^{(I)}$ into the slowness surface for the P wave, Eq. (15). On substitution of the values of $S_z^{(P)}$ and $S_y^{(P)}$ into Eq. (30), the values of the unit vector of particle displacement along the y and z axes for the reflected P wave, $P_y^{(P)}$ and $P_z^{(P)}$, are determined. The values of the coefficients for $A^{(P)}$ in Eq. (28) are thus obtained. The values of the amplitudes of the reflected SV and P waves, $A^{(SV)}$ and $A^{(P)}$, are then obtained by solving Eq. (28) with the thus-determined values of the coefficients for $A^{(SV)}$ and $A^{(P)}$ in Eq. (28) for a given incident SV wave. By varying the angle of incidence of the incident wave. By varying the angle of incidence of the incident SV wave of unit amplitude and by repeating the procedures described above, the amplitude ratios of the reflected SV and P waves to the the incident SV wave are obtained as functions of the angle of incidence. For an incident SV wave in the unidirectional fiberglass epoxy composite as shown in Fig. 1, the amplitude ratios of the reflected SV and P waves to the incident SV wave versus the angle of incidence are plotted in Fig. 5 from zero to the critical angle 52°.

5. Existence of Reflected Surface Wave for Angle of Incidence Equal to or Greater Than Critical Angle

It is seen from Fig. 5 that at the critical angle 52°, the amplitude ratio of the reflected SV wave to the incident SV wave is minus one and the amplitude ratio of the reflected P wave to the incident SV wave is -2.98 instead of being equal to zero. This suggests the possibility of the existence of a surface wave travelling parallel to the plane boundary for the angle of incidence equal to or greater than the critical angle. In the case of an incident SV wave in a semi-infinite isotropic medium with an angle of incidence greater than the critical angle, there exist a reflected SV wave and a surface P wave whose amplitude decays exponentially with the perpendicular distance from the plane boundary [4].

Consider an SV wave travelling in the plane $x = 0$ in the semi-infinite transversely isotropic medium which is incident on the plane boundary, with the angle of incidence equal to or greater than the critical angle. Assume that there exists a surface wave travelling parallel to the plane boundary; that is, the x-component and the z-component of its slowness vector, S_x and S_z, vanish, whereas the y-component of its slowness vector, S_y,

does not vanish, as shown in Fig. 6(a). Let the reflected surface wave be represented as

$$(u, v, w) = A^{(S)}\exp(-C_1 z)(P_x^{(S)}, P_y^{(S)}, P_z^{(S)})$$
$$\exp\{i\omega(S_y^{(S)}y - t)\} \tag{31}$$

where $P_x^{(S)}$, $P_y^{(S)}$ and $P_z^{(S)}$ are the components of a unit vector of particle displacement of the reflected surface wave along the x, y and z axes, respectively; $A^{(S)}$ is the amplitude of particle displacement of the reflected surface wave; $S_y^{(S)}$ is the y-component of the slowness vector of the reflected surface wave; and C_1 is an undetermined real constant which is equal to or greater than zero.

Now, rearrange Eq. (31) into the following form:

$$(u, v, w) = A^{(S)}(P_x^{(S)}, P_y^{(S)}, P_z^{(S)})$$
$$\exp\{i\omega[S_y^{(S)}y + i(C_1/\omega)z] - t\} \tag{32}$$

On substitution of Eq. (32) into Eq. (11), we find that

$$P_x^{(S)} = 0$$
$$[C_{11}S_y^{(S)2} - C_{44}(C_1/\omega)^2 - \rho]P_y^{(S)}$$

$$+ (C_{13} + C_{44})S_y^{(S)} i(C_1/\omega)P_z^{(S)} = 0 \qquad (33)$$

$$(C_{13} + C_{44})S_y^{(S)} i(C_1/\omega)P_y^{(S)}$$

$$+ [C_{44}S_y^{(S)2} - C_{33}(C_1/\omega)^2 - \rho]P_z^{(S)} = 0$$

The condition for the existence of non-trivial solutions for $P_y^{(S)}$ and $P_z^{(S)}$ is expressed by setting the determinant of the matrix of the coefficients of $P_y^{(S)}$ and $P_z^{(S)}$ in Eq. (33) equal to zero:

$$\begin{vmatrix} [C_{11}S_y^{(S)2} - C_{44}(C_1/\omega)^2 - \rho] & (C_{13} + C_{44})S_y^{(S)} i(C_1/\omega) \\ (C_{13} + C_{44})S_y^{(S)} i(C_1/\omega) & [C_{44}S_y^{(S)2} - C_{33}(C_1/\omega)^2 - \rho] \end{vmatrix} = 0 \qquad (34)$$

Expanding Eq. (34), we obtain

$$C_{33}C_{44}\left[(C_1/\omega)^2\right]^2 + \left[C_{33}(\rho - C_{11}S_y^{(S)2}) + C_{44}(\rho - C_{44}S_y^{(S)2}) + (C_{13} + C_{44})^2 S_y^{(S)2}\right](C_1/\omega)^2 + (\rho - C_{11}S_y^{(S)2})(\rho - C_{44}S_y^{(S)2}) = 0 \qquad (35)$$

Eq. (35) is a quadratic equation in $(C_1/\omega)^2$; designate its

coefficients as follows:

$$A = C_{33}C_{44}$$

$$B = C_{33}(\rho - C_{11}S_y^{(S)2}) + C_{44}(\rho - C_{44}S_y^{(S)2}) + (C_{13} + C_{44})^2 S_y^{(S)2} \tag{36}$$

$$C = (\rho - C_{11}S_y^{(S)2})(\rho - C_{44}S_y^{(S)2})$$

It is apparent from Eq. (36) that A is always positive.

By definition, at the critical angle, the angle of reflection of the reflected P wave θ_P is equal to 90° [4]; accordingly, $S_z^{(P)}$ in Eq. (20) is equal to zero. Therefore, the value of b in Eq. (16) corresponding to the critical angle is thus determined by setting S_x and S_z in Eq. (15) equal to zero, and is found to be $(\rho/C_{11})^{1/2}$. As stated following Eq. (19), the angle of reflection of the reflected SV wave θ_{SV} is equal to 90° when the SV wave is tangentially incident on the plane boundary; accordingly, $S_z^{(SV)}$ in Eq. (18) is equal to zero. Therefore, the value of b in Eq. (16) corresponding to the incident SV wave whose slowness vector is parallel to the plane boundary and is in the plane x = 0 is determined by setting S_x and S_z in Eq. (14) equal to zero, and is found to be $(\rho/C_{44})^{1/2}$. The necessary condition for the occurrence of the critical angle phenomenon for an SV

wave travelling in the plane x = 0 is that the value of $(\rho/C_{44})^{1/2}$ has to be greater than that of $(\rho/C_{11})^{1/2}$ [5]. Take numerical values of $(\rho/C_{44})^{1/2}$ and $(\rho/C_{11})^{1/2}$ for the unidirectional fiberglass epoxy composite shown in Fig. 1 from [1] as follows: $(\rho/C_{11})^{1/2} = 0.418$(s/km) and $(\rho/C_{44})^{1/2} = 0.647$(s/km), as shown in Fig. 3. Therefore, these values satisfying the necessary condition on the occurrence of the critical angle phenomenon for an incident SV wave in the unidirectional fiberglass epoxy composite.

It has been shown [5] that when the angle of incidence of an incident SV wave travelling in the plane x = 0 is equal to or greater than the critical angle, the value of b in Eq. (16) lies between $(\rho/C_{11})^{1/2}$ and $(\rho/C_{44})^{1/2}$, that is; $(\rho/C_{11})^{1/2} \leq b \leq (\rho/C_{44})^{1/2}$, as shown in Fig. 3. In addition, it follows from Eq. (5) that the y-component of the slowness vector of the reflected surface wave, $S_y^{(S)}$, is equal to b in Eq. (16). As a result, the value C in Eq. (36) is equal to or less than zero when the angle of incidence of an incident SV wave travelling in the plane x = 0 is equal to or greater than the critical angle; that is, $C \leq 0$. Accordingly, the value of $B^2 - 4AC$ defined in Eq. (36) is equal to or greater than zero for the angle of incidence equal to or greater than the critical angle; that is,

$$B^2 - 4AC = B^2 + 4A|C| \geq 0 \tag{37}$$

Thus, the possible solutions to the quadratic equation in $(C_1/\omega)^2$ in Eq. (35).are

$$(C_1/\omega)^2 = \frac{-B \pm (B^2 - 4AC)^{1/2}}{2A} \tag{38}$$

However, it follows from Eq. (37) that the value of B^2 -4AC is equal to or greater than that of B^2 for any angle of incidence equal to or greater than the critical angle. Consequently, the solution to $(C_1/\omega)^2$, from Eq. (38), is

$$(C_1/\omega)^2 = \frac{-B + (B^2 - 4AC)^{1/2}}{2A} \geq 0 \tag{39}$$

Accordingly, there exists a real constant C_1 given in Eq. (31) when the angle of incidence of the incident SV wave travelling in the plane x = 0 is equal to or greater than the critical angle, and is expressed from Eq. (39), as

$$C_1 = \omega\left[\frac{-B + (B^2 - 4AC)^{1/2}}{2A}\right] \geq 0 \tag{40}$$

The existence of a real constant C_1 in Eq. (40) confirms the existence of the surface wave assumed in Eq. (31).

It is therefore concluded that when the angle of incidence of

an incident SV wave travelling in the unidirectional fiberglass epoxy composite as shown in Fig. 1 is equal to or greater than the critical angle, only an SV wave is reflected back into the medium, and the reflected P wave degenerates into a surface wave which travels parallel to the plane boundary and whose amplitude decreases exponentially with perpendicular distance form the plane boundary, as shown in Fig. 6(b).

6. Balance in Energy Flux Normal to Plane Boundary

The balance in energy flux normal to the plane boundary must be satisfied [2]. For the angle of incidence less than the critical angle, the balance in energy flux normal to the plane boundary $z = 0$, as shown in Fig. 2, is expressed as [2]

$$F_z^{(I)} + F_z^{(P)} + F_z^{(SV)} = 0 \tag{41}$$

where $F_z^{(I)}$, $F_z^{(SV)}$ and $F_z^{(P)}$ are the z-components of the energy fluxes of the incident SV wave, the reflected SV wave and the reflected P wave, respectively.

The z-component of the energy flux of an incident SV wave of unit amplitude travelling in the plane $x = 0$ is [6]

$$F_z^{(I)} = \omega^2(C_{44}P_y^{(I)2}S_z^{(I)} + C_{13}P_y^{(I)}P_z^{(I)}S_y^{(I)} + C_{44}P_y^{(I)}P_z^{(I)}S_y^{(I)} + C_{33}P_z^{(I)2}S_z^{(I)}) \quad (42)$$

Similarly, the z-components of the energy fluxes of the reflected SV and the reflected P waves are [6]

$$F_z^{(P)} = A^{(P)2}\omega^2(C_{44}P_y^{(P)2}S_z^{(P)} + C_{13}P_y^{(P)}P_z^{(P)}S_y^{(P)} + C_{44}P_y^{(P)}P_z^{(P)}S_y^{(P)} + C_{33}P_z^{(P)2}S_z^{(P)}) \quad (43)$$

and

$$F_z^{(SV)} = A^{(SV)2}\omega^2(C_{44}P_y^{(SV)2}S_z^{(SV)} + C_{13}P_y^{(SV)}P_z^{(SV)}S_y^{(SV)} + C_{44}P_y^{(SV)}P_z^{(SV)}S_y^{(SV)} + C_{33}P_z^{(SV)2}S_z^{(SV)}) \quad (44)$$

Since the frequency term ω^2 is common to Eqs. (42), (43) and (44), the balance in energy flux normal to the plane boundary, Eq. (41), is not affected by assuming the value of the frequency ω to be equal to unity. Accordingly, subsequent calculations of the values of the z-components of the energy fluxes of the incident SV wave and the reflected SV and P waves, $F_z^{(I)}$, $F_z^{(SV)}$ and $F_z^{(P)}$, are done by assuming the radian frequency ω to be equal to one.

The value of the z-components of the energy fluxes in Eqs. (42) ,(43) and (44) are obtained similarly to the calculations of the amplitude ratios of the reflected P and SV waves to the incident SV wave for the angle of incidence less than the critical angle. For a given incident SV wave of unit amplitude, the y-components of the slowness vector and of unit vectors of particle displacement, $S_y^{(I)}$, $S_y^{(SV)}$, $S_y^{(P)}$, $P_y^{(I)}$, $P_y^{(SV)}$ and $P_y^{(P)}$, and the z-component of the slowness vectors and of the unit vectors of particle displacement, $S_z^{(I)}$, $S_z^{(SV)}$, $S_z^{(P)}$, $P_z^{(I)}$, $P_z^{(SV)}$ and $P_z^{(P)}$ of the incident SV wave and the reflected SV and P waves are determined first. Then combining the amplitudes of the reflected SV and P waves, $A^{(SV)}$ and $A^{(P)}$, with the values of $S_y^{(I)}$, $S_y^{(SV)}$, $S_y^{(P)}$, $S_z^{(I)}$, $S_z^{(SV)}$, $S_z^{(P)}$, $P_y^{(I)}$, $P_y^{(SV)}$, $P_y^{(P)}$, $P_z^{(I)}$, $P_z^{(SV)}$ and $P_z^{(P)}$, the values of the z-components of the energy fluxes of the incident SV wave and the reflected SV and P waves, $F_z^{(I)}$, $F_z^{(SV)}$ and $F_z^{(P)}$, are thus obtained from Eqs. (42), (43) and (44).

For an SV wave of unit amplitude travelling in the plane x = 0 in the unidirectional fiberglass epoxy composite shown in Fig. 1 incident on a plane boundary, the z-components of the energy fluxes of the reflected SV and P waves and the energy flux of the incident SV wave are plotted in Fig. 7 from zero to the critical angle 52°, with the value of the frequency ω in Eqs. (42), (43)

and (44) equal to one. The balance in energy flux normal to the plane boundary, Eq. (41), is also checked and is shown in Fig. 7.

When the angle of incidence of an incident SV is equal to or greater than the critical angle, only an SV wave is reflected back into the medium with its amplitude ratio to the incident SV equal to minus one, and the reflected P wave degenerates into a surface wave whose energy flux is parallel to the plane boundary [6]. As a result, the energy flux normal to the plane boundary due to the surface wave is equal to zero. The balance in energy flux normal to the plane boundary $z = 0$, as shown in Fig. 6(a), for the angle of incidence equal to or greater than the critical angle is expressed as [2]

$$F^{(I)} + F^{(SV)} = 0 \tag{45}$$

The relationships between the components of the unit vector of particle displacement of an incident SV wave travelling in the plane $x = 0$ along the y and z axes, $P_y^{(I)}$ and $P_z^{(I)}$, and those of the reflected SV wave can be obtained by substituting Eqs. (16) and (17) into Eq. (29) and can be expressed as

$$\begin{aligned} P_y^{(I)} &= P_y^{(SV)} \\ P_z^{(I)} &= -P_z^{(SV)} \end{aligned} \tag{46}$$

On substitution of Eqs. (16), (17) and (46) into Eqs. (42) and (44), it is found that

$$F_z^{(I)} = -F_z^{(SV)} \tag{47}$$

Accordingly, the balance in energy flux normal to the plane boundary, Eq (45), is satisfied when the angle of incidence of an incident SV wave is equal to or greater than the critical angle.

ACOUSTO-ULTRASONIC NON-CONTACT INPUT-OUTPUT CHARACTERIZATION OF UNIDIRECTIONAL FIBERGLASS EPOXY COMPOSITE PLATE

It has been shown that the unidirectional fiberglass epoxy composite shown in Fig. 1 may be modelled as a homogeneous transversely isotropic continuum. For the axes shown in Fig. 1, the isotropic plane of the equivalent continuum lies in the midplane of the plate [1]. A cartesian coordinate system (x, y, z) is chosen so that the x-y plane is the isotropic plane; thus, the upper and lower faces are at $z = h/2$ and $z = -h/2$, respectively, where h is the plate thickness. The properties of the equivalent continuum model of the unidirectional fiberglass epoxy composite plate to be considered are [1]

$$\begin{aligned} h &= 0.1 \text{ m} \\ C_{11} &= 10.581 \times 10^9 \text{ N/m}^2 \\ C_{13} &= 4.67 \times 10^9 \text{ N/m}^2 \\ C_{33} &= 40.741 \times 10^9 \text{ N/m}^2 \\ C_{44} &= 4.422 \times 10^9 \text{ N/m}^2 \\ C_{66} &= 3.243 \times 10^9 \text{ N/m}^2 \\ \rho &= 1850 \text{ kg/m}^3 \end{aligned} \tag{48}$$

Non-contact transmitting and receiving transducers are located on the same face of a fiberglass epoxy composite plate

specimen, as shown in Fig. 8. The unidirectional fiberglass epoxy composite plate specimen is considered as a plate of thickness h and of infinite planar (x-y) extent. The input electrical voltage to the transmitting transducer is $V_i(t)$ and the output electrical voltage from the receiving transducer is $V_o(t)$ where t represents time. The transmitting transducer converts an input electrical voltage into a stress, whereas the receiving transducer converts a displacement associated with stress waves travelling in the plate into an output electrical voltage. In the following analysis, only the SV waves are traced. The SV waves which are generated by the transmitting transducer located above point O experience multiple reflection at each face of the plate, and then reach the receiving transducer located above point M, as shown in Fig. 9. Since the isotropic plane lies in the midplane and is parallel to both the top and bottom faces where the multiple reflections occur, the angle of reflection of the reflected SV wave is equal to the angle of incidence of an incident SV wave for each reflection at each face of the plate. Accordingly, the SV waves travelling from the input O to the output M may be considered as waves propagating in a semi-infinite transversely isotropic medium and travelling to point M′ as if there were no bottom face, as shown in Fig. 9.

1. Delay Time and Phase Velocity

Let the input O and the output M lie in the y-z plane. Assume the number of reflections at the bottom face experienced by the SV wave in travelling from the input O to the output M is n, as shown in Fig. 9. With respect to the z axis, the angle of incidence of the SV wave at each face of the plate is θ, and the total distance travelled by the wave is R_n. From the geometry in Fig. 9,

$$\theta = \tan^{-1}(\ell/2nh) \tag{49}$$

where ℓ is the separation distance between the input O and the output M,

$$R_n = \ell/\sin\theta \tag{50}$$

The delay time t_n for the SV wave to reach the receiving transducer is

$$t_n = R_n/C_1(\theta) \tag{51}$$

where $C_1(\theta)$ is the directionally-dependent phase velocity of the SV wave. The phase velocity C_1 of an SV wave in the unidirectional fiberglass epoxy composite plate is [1]

$$C_1(\theta) = [(C_{44} + C_{11}\sin^2\theta + C_{33}\cos^2\theta - \sqrt{E})/2\rho]^{1/2} \tag{52}$$

where

$$E = [(C_{11} - C_{44})\sin^2\theta + (C_{44} - C_{33})\cos^2\theta]^2 + 4(C_{13} + C_{44})^2\sin^2\theta\cos^2\theta \ ;$$

C_{11}, C_{13}, C_{33}, C_{44} and ρ are given by Eq. (48).

The phase velocity C_1 as a function of the angle of incidence θ is shown in Fig. 10.

The delay time is then computed when the number of reflections n at the bottom face of the plate is equal to 10, 100, 300 or 500. The numerical results are shown in Fig. 11 where the delay time t_n is plotted as the ordinate, and the dimensionless separation ℓ/h is plotted as the abscissa, for values of zero to 300.

2. Displacements Detected by Receiving Transducer

The displacements detected by the non-contact receiving transducer above point M, radiated by the non-contact transmitting transducer, are assumed to be equivalent to the displacement at point M′ associated with the SV wave propagating in a semi-infinite transversely isotropic medium. Except for the reflection coefficients at each face (to be discussed later), the displacement is computed as if there were no bottom boundary, as shown in

Fig. 9. The displacement at point M′ is approximated by the far-field asymptotic solution for large R_n of an infinite transversely isotropic medium subjected to a harmonic point force.

Consider an infinite transversely isotropic medium in which the z axis of a rectangular cartesian coordinate system O(x, y, z) is the zonal axis of the medium, and the x-y plane coincides with isotropic plane, as shown in Fig. 12. The equations of motion including the body force are [7]

$$\tau_{xx,x} + \tau_{xy,y} + \tau_{xz,z} + \rho X = \rho u,tt \tag{53}$$

$$\tau_{xy,x} + \tau_{yy,y} + \tau_{yz,z} + \rho Y = \rho v,tt \tag{54}$$

$$\tau_{xz,x} + \tau_{yz,y} + \tau_{zz,z} + \rho Z = \rho w,tt \tag{55}$$

where τ_{rs} (r, s = x, y and z) are the normal (r = s) and shear ($r \neq s$) stresses with respect to the chosen coordinate system O(x, y, z); u, v and w are displacement components of a point in the medium along the x, y and z axes, respectively; X, Y and Z are the components of the body force along the x, y and z axes, respectively; ρ is the density; t is time ; and "," denotes partial differentiation with respect to the variable which follows.

Combining Eqs. (1) and (55) gives

$$\Gamma,tt = \left(\frac{C_{13} + C_{44}}{\rho}\right) \Delta,zz + \left(\frac{C_{44}}{\rho}\right) \Gamma,xx + \left(\frac{C_{44}}{\rho}\right) \Gamma,yy + \left(\frac{C_{33}}{\rho}\right) \Gamma,zz + Z,z \tag{56}$$

where Γ and Δ are given by [6]

$$\Gamma = w,z \quad \text{and} \quad \Delta = u,x + v,y \ .$$

By differentiating Eq. (53) with respect to x and Eq. (54) with respect to y, we find, on addition of the resulting equations and using the appropriate stress-strain relation, Eq. (1), that

$$\Delta,tt = \left(\frac{C_{13} + C_{44}}{\rho}\right) (\Gamma,xx + \Gamma,yy) + \frac{C_{44}}{\rho} \Delta,zz + \frac{C_{11}}{\rho} (\Delta,xx + \Delta,yy) + X,x + Y,y \tag{57}$$

For a harmonic point force at the origin, the body forces may be taken of the form [7]

$$X = X_o \delta(x)\delta(y)\delta(z)e^{-i\omega t}$$

$$Y = Y_o \delta(x)\delta(y)\delta(z)e^{-i\omega t} \tag{58}$$

$$Z = Z_o \delta(x)\delta(y)\delta(z)e^{-i\omega t}$$

where $\delta(r)$ ($r = x$, y and z) is the Dirac delta function.

Express Γ and Δ as threefold Fourier Integrals [7] as follows:

$$\Gamma(x,y,z,t) = \int_{-\infty}^{\infty}\int\int\int \bar{\Gamma}(S_x,S_y,S_z,t)$$

$$\exp\{i\omega(S_x x + S_y y + S_z z - t)\}dS_x dS_y dS_z \qquad (59)$$

$$\Delta(x,y,z,t) = \int_{-\infty}^{\infty}\int\int\int \bar{\Delta}(S_x,S_y,S_z,t)$$

$$\exp\{i\omega(S_x x + S_y y + S_z z - t)\}dS_x dS_y dS_z$$

where

$$\bar{\Gamma}(S_x,S_y,S_z,t) = 1/8\pi^3 \int_{-\infty}^{\infty}\int\int\int \Gamma(x,y,z,t)$$

$$\exp\{i\omega(-S_x x - S_y y - S_z z + t)\}dxdydz.$$

$$\bar{\Delta}(S_x,S_y,S_z,t) = 1/8\pi^3 \int_{-\infty}^{\infty}\int\int\int \Delta(x,y,z,t)$$

$$\exp\{i\omega(-S_x x - S_y y - S_z z + t)\}dxdydz.$$

Similarly, X,x, Y,y and Z,z can be expressed as threefold Fourier integrals

$$X,x = i\omega S_x \iiint_{-\infty}^{\infty} \bar{X} \exp\{i\omega(S_x x + S_y y + S_z z - t)\} dS_x dS_y dS_z \tag{60}$$

$$Y,y = i\omega S_y \iiint_{-\infty}^{\infty} \bar{Y} \exp\{i\omega(S_x x + S_y y + S_z z - t)\} dS_x dS_y dS_z \tag{61}$$

$$Z,z = i\omega S_z \iiint_{-\infty}^{\infty} \bar{Z} \exp\{i\omega(S_x x + S_y y + S_z z - t)\} dS_x dS_y dS_z \tag{62}$$

where

$$\bar{X} = 1/8\pi^3 \iiint_{-\infty}^{\infty} X_o \delta(x)\delta(y)\delta(z) e^{-i\omega t}$$

$$\exp\{i\omega(-S_x x - S_y y - S_z z + t)\} dS_x dS_y dS_z = X_o/8\pi^3$$

and, similarly, $\bar{Y} = Y_o/8\pi^3$; $\bar{Z} = Z_o/8\pi^3$.

Substitution of Eqs. (58) through (62) into Eqs. (56) and (57) gives

$$\bar{\Delta} = \frac{C_{44}/\rho(S_x^2 + S_y^2) + C_{33}/\rho S_z^2 - 1}{8\pi^3\omega H(S_x, S_y, S_z)} (iS_xX_o + iS_yY_o)$$

$$+ \frac{-(C_{13} + C_{44})/\rho\ (S_x^2 + S_y^2)}{8\pi^3\omega H(S_x, S_y, S_z)} iS_zZ_o \tag{63}$$

$$\bar{\Gamma} = \frac{-(C_{13} + C_{44})/\rho\ S_z^2}{8\pi^3\omega H(S_x, S_y, S_z)} (iS_xX_o + iS_yY_o)$$

$$+ \frac{C_{11}/\rho(S_x^2 + S_y^2) + C_{33}/\rho S_z^2 - 1}{8\pi^3\omega H(S_x, S_y, S_z)} iS_zZ_o \tag{64}$$

where

$$H(S_x, S_y, S_z) = \left[\frac{C_{44}}{\rho} S_z^2 + \frac{C_{11}}{\rho} (S_x^2 + S_y^2) - 1\right]$$

$$\left[\frac{C_{44}}{\rho}(S_x^2 + S_y^2) + \frac{C_{33}}{\rho}S_z^2 - 1\right] \tag{65}$$

$$- \left(\frac{C_{44} + C_{13}}{\rho}\right)^2 S_z^2(S_x^2 + S_y^2)$$

In fact, $H(S_x, S_y, S_z) = 0$ represents the two sheets of slowness surface, one for a P wave and one for an SV wave [8]. As a result of Eqs. (63) and (64),

$$\Gamma(x,y,z,t) = \int_{-\infty}^{\infty}\int\int\int \left[\left[\frac{-(C_{13} + C_{44})/\rho\ S_z^2}{8\pi^3\omega H(S_x,S_y,S_z)}\right](iS_xX_o + iS_yY_o)\right.$$

$$\left. + \left[\frac{C_{11}/\rho(S_x^2 + S_y^2) + C_{33}/\rho S_z^2 - 1}{8\pi^3\omega H(S_x,S_y,S_z)}\right] iS_zZ_o\right] \tag{66}$$

$$\exp\{i\omega(S_xx + S_yy + S_zz - t)\}$$

$$\Delta(x,y,z,t) = \int_{-\infty}^{\infty}\int\int\int \left[\left[\frac{C_{44}/\rho(S_x^2 + S_y^2) + C_{33}/\rho S_z^2 - 1}{8\pi^3\omega H(S_x,S_y,S_z)}\right](iS_xX_o + iS_yY_o)\right.$$

$$\left. + \left[\frac{-(C_{13} + C_{44})/\rho\ (S_x^2 + S_y^2)}{8\pi^3\omega H(S_x,S_y,S_z)}\right] iS_zZ_o\right] \tag{67}$$

$$\exp\{i\omega(S_xx + S_yy + S_zz - t)\}$$

The asymptotic solution at a large distance from the point force is obtained by applying the theory of residues, the method of stationary phase, and the radiation condition [8] as

$$\Gamma(x,y,z,t) = \sim \frac{\omega}{2\pi R}\sum_{n=1}^{N} A_n\lambda_n \left[\frac{-(C_{13}+C_{44})}{\rho}\ S_{zn}^2(iS_{xn}X_o+iS_{yn}Y_o)\right.$$

$$\left. + \left[\frac{C_{11}}{\rho}\ (S_{xn}^2 + S_{yn}^2) + \frac{C_{33}}{\rho}\ S_{zn}^2 - 1\right] iS_{zn}Z_o\right] \tag{68}$$

$$\exp\{i\omega(S_{xn}x + S_{yn}y + S_{zn}z - t)\}$$

$$\Delta(x,y,z,t) = -\frac{\omega}{2\pi R}\sum_{n=1}^{N} A_n\lambda_n \left\{\left[\frac{C_{44}}{\rho}(S_{xn}^2 + S_{yn}^2) + \frac{C_{33}}{\rho} S_{zn}^2 - 1\right]\right.$$

$$\left.(iS_{xn}X_o + iS_{yn}Y_o) + \frac{-(C_{13}+C_{44})}{\rho}(S_{xn}^2 + S_{yn}^2)\, iS_{zn}Z_o\right\}$$

$$\exp\{i\omega(S_{xn}x + S_{yn}y + S_{zn}z - t)\} \qquad (69)$$

where R is the distance from the origin O where the point forces are applied to the location of interest Q in the medium, as shown in Fig. 12; (S_{xn}, S_{yn}, S_{zn}) are points on the slowness surface for an SV wave where the normal is parallel to the OQ direction; N is the total number of points (S_{xn}, S_{yn}, S_{zn}) are points over which the summation must be performed ; λ_n is the amplitude coefficient and is given by

$$\lambda_n = \left\{\frac{H,S_x^2 + H,S_y^2 + H,S_z^2}{|K_n|}\right\}^{1/2} \qquad (70)$$

where K_n is given as

$$k_n = \Sigma\,[H,S_z^2(H,S_xS_x\ H,S_yS_y - H,S_xS_y^2) + 2H,S_x\ H,S_y(H,S_xS_z\ H,S_yS_z - H,S_xS_y\ H,S_zS_z)] \qquad (71)$$

where Σ denotes the sum with respect to cyclic permutation of S_x, S_y and S_z; the symbol $|\ |$ denotes "the magnitude of"; λ_n is evaluated at points (S_{xn}, S_{yn}, S_{zn}) on the slowness surface for

an SV wave where the normal is parallel to the OQ direction, exclusive of those singular points (S_{xn}, S_{yn}, S_{zn}) resulting in K_n in Eq. (71) equal to zero; and A_n is the phase constant and is determined as follows: $A_n = 1$ if $K_n > 0$ or $A_n = i$ if $K_n < 0$.

The displacement components along the x, y and z axes, u, v and w due to an SV wave can be obtained by direct integration of the definition of Γ and Δ in Eq. (56), and are given as [8]

$$u = \frac{S_x}{i\omega(S_x^2 + S_y^2)} \Delta$$

$$v = \frac{S_y}{i\omega(S_x^2 + S_y^2)} \Delta \qquad (72)$$

$$w = \frac{1}{i\omega S_z} \Gamma$$

Substitution of Eqs. (68) and (69) into Eq. (72) gives the asymptotic solutions at a large distance to the displacement components along the x, y and z axes, u, v and w, as follows:

$$u \sim \frac{-i}{2\pi R} \sum_{n=1}^{N} A_n \lambda_n \left\{ \frac{S_{xn}}{(S_{xn}^2 + S_{yn}^2)} \left[\left[\frac{C_{44}}{\rho} (S_{xn}^2 + S_{yn}^2) + \frac{C_{33}}{\rho} S_{zn}^2 - 1 \right] \right.\right.$$

$$\left.\left. (iS_{xn}^2 X_o + iS_{yn}^2 Y_o) + \frac{-(C_{13}+C_{44})}{\rho} (S_{xn}^2 + S_{yn}^2)\ iS_{zn}^2\ Z_o \right] \right.$$

$$\left. \exp\{i\omega(S_{xn}x + S_{yn}y + S_{zn}z - t)\} \right. \qquad (73)$$

$$v \sim \frac{-i}{2\pi R} \sum_{n=1}^{N} A_n \lambda_n \frac{S_{yn}}{(S_{xn}^2 + S_{yn}^2)} \left[\left[\frac{C_{44}}{\rho} (S_{xn}^2 + S_{yn}^2) + \frac{C_{33}}{\rho} S_{zn}^2 - 1 \right] \right.$$

$$\left. (iS_{xn}^2 X_o + iS_{yn}^2 Y_o) + \frac{-(C_{13}+C_{44})}{\rho} (S_{xn}^2 + S_{yn}^2)\, iS_{zn} Z_o \right]$$

$$\exp\{i\omega(S_{xn}x + S_{yn}y + S_{zn}z - t)\} \qquad (74)$$

$$w \sim \frac{1}{2\pi R} \sum_{n=1}^{N} A_n \lambda_n \left[\frac{-(C_{13}+C_{44})}{\rho} S_{zn} (iS_{xn}X_o + iS_{yn}Y_o) \right.$$

$$\left. + \left(\frac{C_{11}}{\rho} (S_{xn}^2 + S_{yn}^2) + \frac{C_{33}}{\rho} S_{zn}^2 - 1 \right) Z_o \right]$$

$$\exp\{i\omega(S_{xn}x + S_{yn}y + S_{zn}z - t)\} \qquad (75)$$

3. Directivity Functions

The shear stress τ_{yz} and the normal stress τ_{zz} associated with the SV waves reaching the point M′ in Fig. 9 are used to study their associated directivity functions. The asymptotic shear stress τ_{yz} and the asymptotic normal stress τ_{zz} are given by substituting Eqs. (68) through (72) into Eq. (1) as

$$\tau_{zz} \sim \frac{\omega}{2\pi R} \sum_{n=1}^{N} A_n \lambda_n \left\{ C_{33} \left[\frac{-(C_{13}+C_{44})}{\rho} S_{zn}^2 (iS_{xn}X_o + iS_{yn}Y_o) \right. \right.$$

$$\left. \left. + \left[\frac{C_{11}}{\rho} (S_{xn}^2 + S_{yn}^2) + \frac{C_{33}}{\rho} S_{zn}^2 - 1 \right] iS_{zn} Z_o \right] + \right.$$

$$C_{13}\left[\left\{\frac{C_{44}}{\rho}(S_{xn}^2 + S_{yn}^2) + \frac{C_{33}}{\rho} S_{zn}^2 - 1\right\}(iS_{xn}X_o + iS_{yn}Y_o)\right.$$

$$\left. + \frac{-(C_{13}+C_{44})}{\rho} (S_{xn}^2 + S_{yn}^2)\, iS_{zn}Z_o\right]\Big\}$$

$$\exp\{i\omega(S_{xn}x + S_{yn}y + S_{zn}z - t)\} \qquad (76)$$

$$\tau_{yz} \sim \frac{C_{55}\omega}{2\pi R} \sum_{n=1}^{N} A_n\lambda_n \left\{S_{yn}\left[\frac{-(C_{13}+C_{44})}{\rho} S_{zn}^2 (iS_{xn}X_o + iS_{yn}Y_o)\right.\right.$$

$$\left. + \left(\frac{C_{11}}{\rho}(S_{xn}^2 + S_{yn}^2) + \frac{C_{33}}{\rho} S_{zn}^2 - 1\right)iZ_o\right]$$

$$+ \frac{S_{yn}S_{zn}}{S_{xn}^2 + S_{yn}^2}\left[\left[\frac{C_{44}}{\rho} (S_{xn}^2 + S_{yn}^2) + \frac{C_{33}}{\rho} S_{zn}^2 - 1\right](iS_{xn}X_o + iS_{yn}Y_o)\right.$$

$$\left.\left. + \frac{-(C_{13}+C_{44})}{\rho} (S_{xn}^2 + S_{yn}^2)\, iS_{zn}Z_o\right]\right\}$$

$$\exp\{i\omega(S_{xn}x + S_{yn}y + S_{zn}z - t)\} \qquad (77)$$

The directivity functions associated with the normal stress τ_{zz} in Eq. (76) and the shear stress τ_{yz} in Eq. (77) will be evaluated for the case of $S_x = 0$. Due to the axial symmetry with respect to the zonal axis, the z axis, of the transversely isotropic medium, the values of the directivity functions thus obtained hold for all values of S_x.

Consider the case of the point force acting along the y

direction only; that is, $Y_o \neq 0$ but $X_o = Z_o = 0$ in Eq. (58).

The directivity function D^Y_{yz} of the shear stress τ_{yz} associated with an SV wave is evaluated from Eq. (77) along the arc $y^2 + z^2 = 1$ in the positive y-z quadrant by setting $Y_o = R = 1$;

$$D^Y_{yz} = \frac{\omega C_{55}}{2\pi} \left| \sum_{n=1}^{N} A_n \lambda_n S_{zn} \left(\frac{-C_{13}}{\rho} S_{yn}^2 + \frac{C_{33}}{\rho} S_{zn}^2 - 1 \right) \exp\{i\omega(S_{yn}y + S_{zn}z)\} \right| \tag{78}$$

where the summation Σ is done vectorially in a complex plane over each type of wave passing a given point (0, y, z) on the arc $y^2 + z^2 = 1$; each wave corresponds to a point (0, S_{yn}, S_{zn}) on the slowness surface of an SV wave at which the normal is parallel to the radius vector of the given point (0, y, z). Similarly, the directivity function D^Y_{zz} of the normal stress τ_{zz} is, from Eq. (76), for $Y_o = R = 1$;

$$D^Y_{zz} = \frac{\omega}{2\pi} \left| \sum_{n=1}^{N} A_n \lambda_n S_{yn} \left[\frac{C_{13}C_{44}}{\rho} S_{yn}^2 - \frac{C_{33}C_{44}}{\rho} S_{zn}^2 - C_{13} \right] \exp\{i\omega(S_{yn}y + S_{zn}z)\} \right| \tag{79}$$

Next, consider the case of the point force acting along the z direction only; that is, $Z_o \neq 0$ but $X_o = Y_o = 0$ in Eq. (58).

Z

The directivity function D_{yz} of the shear stress τ_{yz} associated with an SV wave is evaluated from Eq. (77) along the arc $y^2 + z^2 = 1$ in the positive y-z quadrant by setting $Z_o = R = 1$;

$$D^Z_{yz} = \frac{\omega C_{55}}{2\pi} \left| \sum_{n=1}^{N} A_n \lambda_n S_{yn} \left[\frac{C_{11}}{\rho} S_{yn}^2 + \frac{C_{33} - C_{44} - C_{13}}{\rho} S_{zn}^2 - 1 \right] \right.$$
$$\left. \exp\{i\omega(S_{yn}y + S_{zn}z)\} \right| \qquad (80)$$

Similarly, the directivity function D_{zz} of the normal stress τ_{zz} is, from Eq. (76), for $Z_o = R = 1$;

$$D^Z_{zz} = \frac{\omega}{2\pi} \left| \sum_{n=1}^{N} A_n \lambda_n S_{zn} \left[\frac{C_{11}C_{33} - C_{13}C_{44} - C_{13}^2}{\rho} S_{yn}^2 \right. \right.$$
$$\left. \left. + \frac{C_{33}^2}{\rho} S_{zn}^2 - C_{33} \right] \exp\{i\omega(S_{yn}y + S_{zn}z)\} \right| \qquad (81)$$

Finally, consider the case of the point force acting along the x direction only; that is, $X_o \neq 0$ but $Y_o = Z_o = 0$ in Eq. (58). It follows from Eqs. (76) and (77) that the values of the shear stress τ_{yz} and the normal stress τ_{zz} associated with an SV wave travelling in the plane $x = 0$ are equal to zero.

The polar diagrams for the directivity functions of the shear stress τ_{yz} and the normal stress τ_{zz} (D^Y_{yz}, D^Y_{zz}, D^Z_{yz} and D^Z_{zz} given

in Eqs. (78) through (81)) associated with the SV waves propagating in the unidirectional fiberglass epoxy composite as shown in Fig. 1 are obtained by substituting Eq. (48) into Eqs. (78) through (81) at frequencies of 0.75, 1.50 and 2.25 MHz.

Numerical results are shown in Figs. 13 through 24 where the angle of incidence θ given in Eq. (49) is used to determine the direction in which the values of points $(0, S_{yn}, S_{zn})$ on the slowness surface, where the normal is parallel to the given direction, is thus obtained.

4. Assumptions of Transducers

The non-contact transmitting transducer in Fig. 8 is assumed to transform an electrical voltage into a uniform stress; however, the non-contact receiving transducer in Fig. 8 transforms a displacement into an electrical voltage. The approach below is similar to that given in [9]. Referring to Fig. 8, if an input voltage of amplitude of V and frequency ω is applied according to

$$V_i(t) = Ve^{-i\omega t} \quad . \tag{82}$$

The stress σ that is introduced into the specimen plate by the non-contact transmitting transducer is

$$\sigma(t) = F_1(\omega)Ve^{-i(\omega t + \phi_1)} \tag{83}$$

where $F_1(\omega)$ is the transduction ratio for the non-contact transmitting transducer in transforming a voltage to a stress and ϕ_1 is a phase angle. In Eqs. (82) and (83), the complex harmonic character of the signals is expressed in the complex notation where $i = \sqrt{-1}$ and only the real part of these and subsequent equations should be considered. Thus, the amplitude T of the applied load is defined as

$$T = F_1(\omega)V \tag{84}$$

Similarly, if a stress wave producing a displacement d of amplitude D and frequency ω that is detected by the non-contact receiving transducer is defined as

$$d(t) = De^{-i\omega t} \tag{85}$$

the output voltage from the non-contact receiving transducer, see Fig. 8, is

$$V_o(t) = F_2(\omega)De^{-i(\omega t + \phi_2)} \tag{86}$$

where $F_2(\omega)$ is the transduction ratio for the non-contact receiving transducer in transforming a displacement to a voltage, and ϕ_2 is a phase angle. Thus, the amplitude V′ of the output

electrical voltage is

$$V' = F_2(\omega)D \tag{87}$$

The characteristics of $F_1(\omega)F_2(\omega)$ are unknown except that the dimensions of the product $F_1(\omega)$ are $[kg/m^2 \cdot sec^2]$.

5. Steady-State Output Voltage Amplitude due to Multiple Wave Reflections in Plate

Since the SV wave traced in the unidirectional fiberglass epoxy composite plate specimen shown in Fig. 9 is travelling in the y-z plane, it follows from Eqs. (73), (74) and (75) that only the displacement components along the y and z axes, v and w, are detectable at the point M'. Consider first the point force acting along the y direction only; that is $Y_o \neq 0$ but $X_o = Z_o = 0$ in Eq. (58).

The amplitude of the y-component displacement D_v^Y evaluated at the point M' can be obtained from Eqs. (50) and (74) as

$$D_v^Y = \frac{f_1(S_{yn}, S_{zn})}{R_n} Y_o \tag{88}$$

where

$$f_1(S_{yn}, S_{zn}) = 1/2\pi \left| \sum_{n=1}^{N} A_n\lambda_n[(C_{44}/\rho)S_{yn}^2 + (C_{33}/\rho)S_{zn}^2 - 1] \right.$$
$$\left. \exp\{i\omega(S_{yn}y + S_{zn}z)\} \right|$$

and is evaluated along the arc $y^2 + x^2 = 1$. Similarly, the amplitude of the z-component displacement D_w^Y evaluated at the point M′ can be obtained from Eqs. (50) and (75) as

$$D_w^Y = \frac{f_2(S_{yn}, S_{zn})}{R_n} Y_o \tag{89}$$

where

$$f_2(S_{yn}, S_{zn}) = 1/2\pi \left| \sum_{n=1}^{N} A_n \lambda_n [(C_{13} + C_{44})/\rho] S_{yn} S_{zn} \right.$$

$$\left. \exp\{i\omega(S_{yn} y + S_{zn} z)\} \right| .$$

Next, consider the point force acting along the z direction only; that is $Z_o \neq 0$ but $X_o = Y_o = 0$ in Eq. (58).

The amplitude of the y-component displacement D_v^Z evaluated at the point M′ can be obtained from Eqs. (50) and (74) as

$$D_v^Z = \frac{f_2(S_{yn}, S_{zn})}{R_n} Z_o \tag{90}$$

Similarly, the amplitude of the z-component displacement D_w^Z evaluated at the point M′ can be obtained from Eqs. (50) and (75) as

$$D_w^Z = \frac{f_3(S_{yn}, S_{zn})}{R_n} Z_o \tag{91}$$

where

$$f_3(S_{yn}, S_{zn}) = 1/2\pi \left| \sum_{n=1}^{N} A_n \lambda_n [(C_{11}/\rho) S_{yn}^2 + (C_{33}/\rho) S_{zn}^2 - 1] \right.$$

$$\exp\{i\omega(S_{yn}y + S_{zn}z)\}\Big| \quad .$$

Finally, consider the point force acting along the x direction only; that is, $X_o \neq 0$ but $Y_o = Z_o = 0$ in Eq. (58). It follows from Eqs. (74) and (75) that the amplitude of the y-component displacement and the amplitude of the z-component displacement vanish at the point M′. This is due to the fact that the SV wave is travelling in the y-z plane.

According to Eqs. (88) through (91), the amplitude of a displacement component at the point M′, denoted as $D_{M'}$, can be expressed in the following form as

$$D_{M'} = \frac{f_i(S_{yn}, S_{zn})}{R_n} T \tag{92}$$

where T is the applied point force and is equivalent to either Y_o or Z_o in Eqs. (88) through (91); and $f_i(S_{yn}, S_{zn})$ (i = 1, 2 or 3) is determined from one of Eqs. (88) through (91), depending on which displacement component is measured and along which direction the point load is applied.

However, with the bottom boundary present, the wave is reflected a total of (2n -1) times, as shown in Fig. 9. Thus, the amplitude of displacement at the point M is D_M and is expressed as

$$D_M = Q_{SVSV}^{2n-1} D_{M'} \tag{93}$$

where Q_{SVSV} is the amplitude ratio of the reflected SV wave to the incident SV wave, as shown in Fig. 5, and is a function of the angle of incidence θ defined in Eq. (49). Here, we have ignored the effects of mode conversion.

The amplitude of the output voltage form the non-contact receiving transducer is V′ and can be obtained by substituting Eqs. (92) and (93) into Eq. (87) as

$$V' = \frac{F_2(\omega) Q_{SVSV}^{2n-1} f_i(S_{yn}, S_{zn})}{R_n} T \tag{94}$$

Substitution of Eq. (84) into Eq. (94) gives

$$V' = \frac{F_1(\omega) F_2(\omega) Q_{SVSV}^{2n-1} f_i(S_{yn}, S_{zn})\ V}{R_n} \tag{95}$$

Introducing the SV wave attenuation constant α of the unidirectional fiberglass epoxy composite and a possible electrical signal amplification factor K, Eq. (95) can be written as

$$V' = KF_1(\omega) F_2(\omega) Q_{SVSV}^{2n-1} f_i(S_{yn}, S_{zn}) V \frac{e^{-\alpha Rn}}{R_n} \tag{96}$$

Eq. (96) gives the output voltage amplitude from the non-contact

receiving transducer due to an input voltage amplitude V at the non-contact transmitting transducer when the SV wave path has undergone n reflections from the bottom face of the unidirectional fiberglass epoxy composite plate specimen, as shown in Fig. 9.

DISCUSSION AND CONCLUSION

In the acousto-ultrasonic input-output characterization of the unidirectional fiberglass epoxy composite plate, the angle of reflection of the reflected SV wave is equal to the angle of incidence of the incident SV wave for each reflection at either the top or the bottom face of the plate. This is due to the fact that the isotropic plane is parallel to both faces of the plate. However, if the parallelism between the isotropic plane and the plane boundaries where reflection occurs does not exist, the angle of reflection is not equal to the angle of incidence. In such a case, the use of a semi-infinite transversely isotropic medium, neglecting the existence of the bottom face of the plate except for the cumulative reflection coefficients, to compute the delay time, the displacements and the directivity functions becomes inappropriate.

For an SV wave travelling in an isotropic medium, its phase velocity is a constant value; that is, its phase velocity is directionally independent. However, as shown in Fig. 10, the phase velocity C_1 of an SV wave travelling in a unidirectional fiberglass epoxy composite plate is a function of the angle of incidence θ. Consequently, the directional dependence of the phase velocity of an SV wave in the unidirectional fiberglass

epoxy composite plate has an effect on the delay time when conducting acousto-ultrasonic input-output characterization. This phenomenon can be observed at low values of dimensionless separation ℓ/h in Fig. 11, where sharp increases in delay time t_n are caused by an increase in the number of reflection n from the bottom face of the plate at a given value of the dimensionless separation ℓ/h. Low values of dimensionless separation ℓ/h correspond to an angle of incidence θ (given in Eq. (49)) whose value is less than 60° which is the abscissa of the maximum phase velocity C_1, as shown in Fig. 10. For angles of incidence θ less than 60°, the phase velocity C_1 increases with increasing angle of incidence θ, as shown in Fig. 10. However, an increase in the number of reflections n from the bottom face of the plate for a given plate thickness h and a given separation distance ℓ results in a decrease in the angle of incidence θ given by Eq. (49), thereby increasing the travelling distance R_n according to Eq. (50) and decreasing the accompanying phase velocity. The increase in the travelling distance R_n and the decrease in the phase velocity C_1 account for the sharp increases in the delay time t_n at low values of dimensionless separation ℓ/h. For the case of an SV wave travelling in an isotropic medium, the increase in the delay time t_n caused by an increase in the number of reflections n is attributed solely to the increase in the travelling distance R_n.

Consider the case of a given number of reflections n. For a given plate thickness h, an increase in the separation distance ℓ results in an increases in the travelling distance R_n, as shown in Fig. 9, and an increase in the angle of incidence θ given by Eq. (49). An increase in the angle of incidence θ may result in an increase or a decrease in the SV-wave phase velocity C_1, depending on whether the angle of incidence θ is less than or greater than 60°, as shown in Fig. 10. However, as the separation distance ℓ approaches infinity, the angle of incidence θ will approach 90°, and the phase velocity C_1 will reach a limit, as shown in Fig. 10. Consequently, (for $\ell/h \rightarrow \infty$) the increase in the delay time t_n is due almost exclusively to the increase in the travelling distance R_n, which is similar to the isotropic medium case.

This theoretical investigation provides a step forward in the quantitative understanding of acousto-ultrasonic nondestructive evaluation (NDE) parameters such as the stress wave factor (SWF) in transversely isotropic media. It also provides the potential for assisting in the development of more efficient and more revealing NDE schemes utilizing wave propagation.

REFERENCES

[1] E. R. C. Marques and J. H. Williams, Jr., "Stress Waves in Transversely Isotropic Media," Composite Materials and Nondestructive Evaluation Laboratory, M.I.T., May 1986.

[2] E. G. Henneke II, "Reflection-Refraction of a Stress Wave at a Plane Boundary between Anisotropic Media," Journal of Acoustical Society of America, Vol. 51, Part 2, April 1972, pp. 210-217.

[3] M. J. P. Musgrave, "On the Propagation of Elastic Waves in Anisotropic Media," Proceedings of the Royal Society of London, Series A, Vol. 225, 1954, pp. 339-355.

[4] K. F. Graff, Wave Motion in Elastic Solids, Ohio State University, Columbus, 1975, pp. 320-321.

[5] M. J. P. Musgrave, " The Propagation of Elastic Waves in Crystals and Other Anisotropic Media," Report on Progress in Physics, Vol. 22, 1959, pp. 74-96.

[6] M. J. P Musgrave, "Reflection and Refraction of Plane Elastic Waves at a Plane Boundary between Aeolotropic Media," Journal of Geophysics, Vol. 3, 1960, pp. 406-418.

[7] V. T. Buchwald, "Elastic Waves in Anisotropic Media," Proceeding of the Royal Society, Series A, Vol. 253, 1959, pp. 563-580.

[8] J. H. Williams, Jr., E. R. C. Marques and S. S. Lee, " Wave Propagation in Anisotropic Infinite Medium Due to an Oscillatory Point Source with Application to a Unidirectional Composite Material," Composite Materials and Nondestructive Evaluation Laboratory, M.I.T., May 1986.

[9] J. H. Williams, Jr., H. Karagulle and S. S. Lee, "Ultrasonic Input-Output for Transmitting and Receiving Longitudinal Transducers Coupled to Same Face of Isotropic Elastic Plate," Material Evaluation, Vol. 40, May 1982, pp. 655-662.

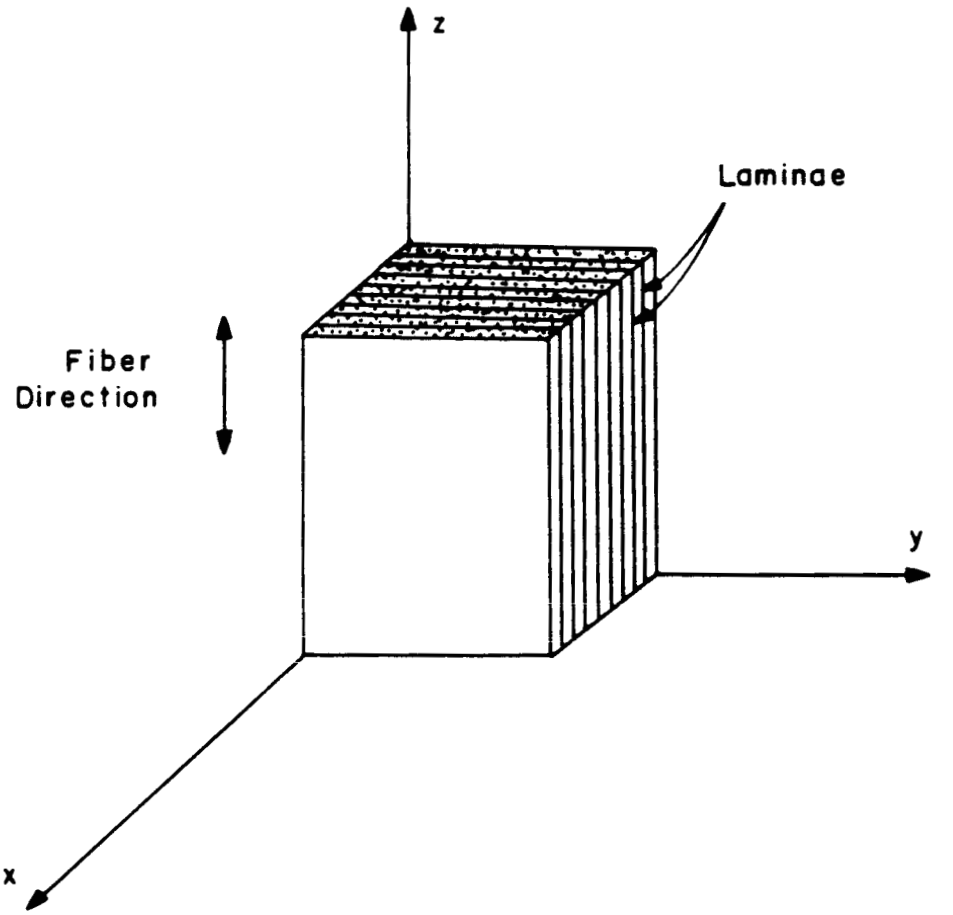

Fig. 1 Unidirectional fiber reinforced composite modelled as transversely isotropic medium.

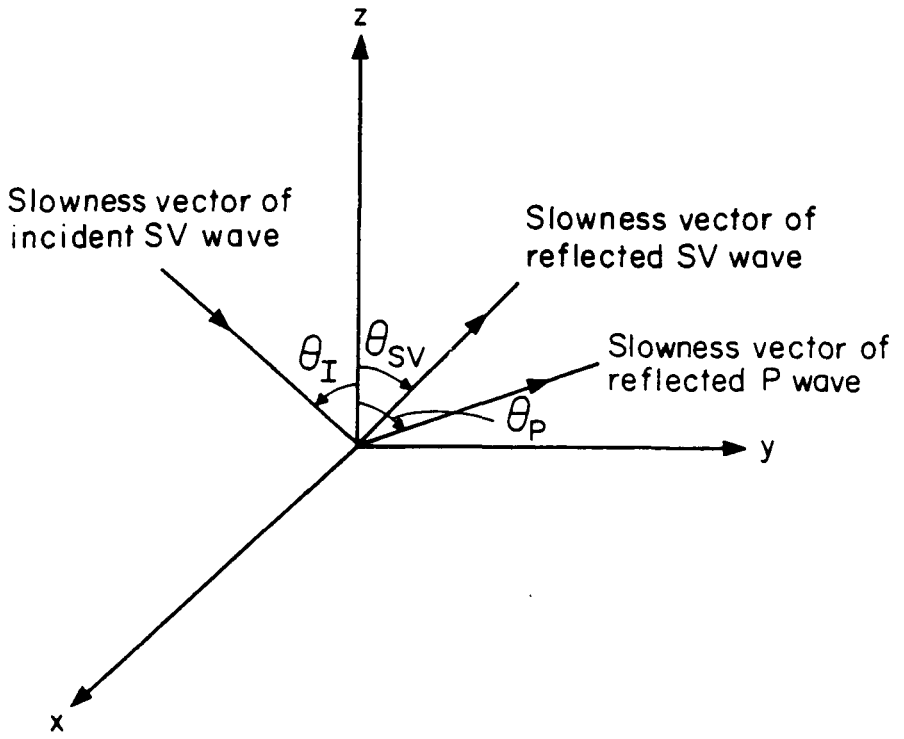

Fig. 2 Coordinate system (x,y,z) in the analysis of single reflection problem at stress-free plane boundary of semi-infinte transversely isotropic medium for angle of incidence less than critical angle; $z = 0$ is plane boundary where single reflection occurs, $z < 0$ is free space, and $x = 0$ is plane of incidence.

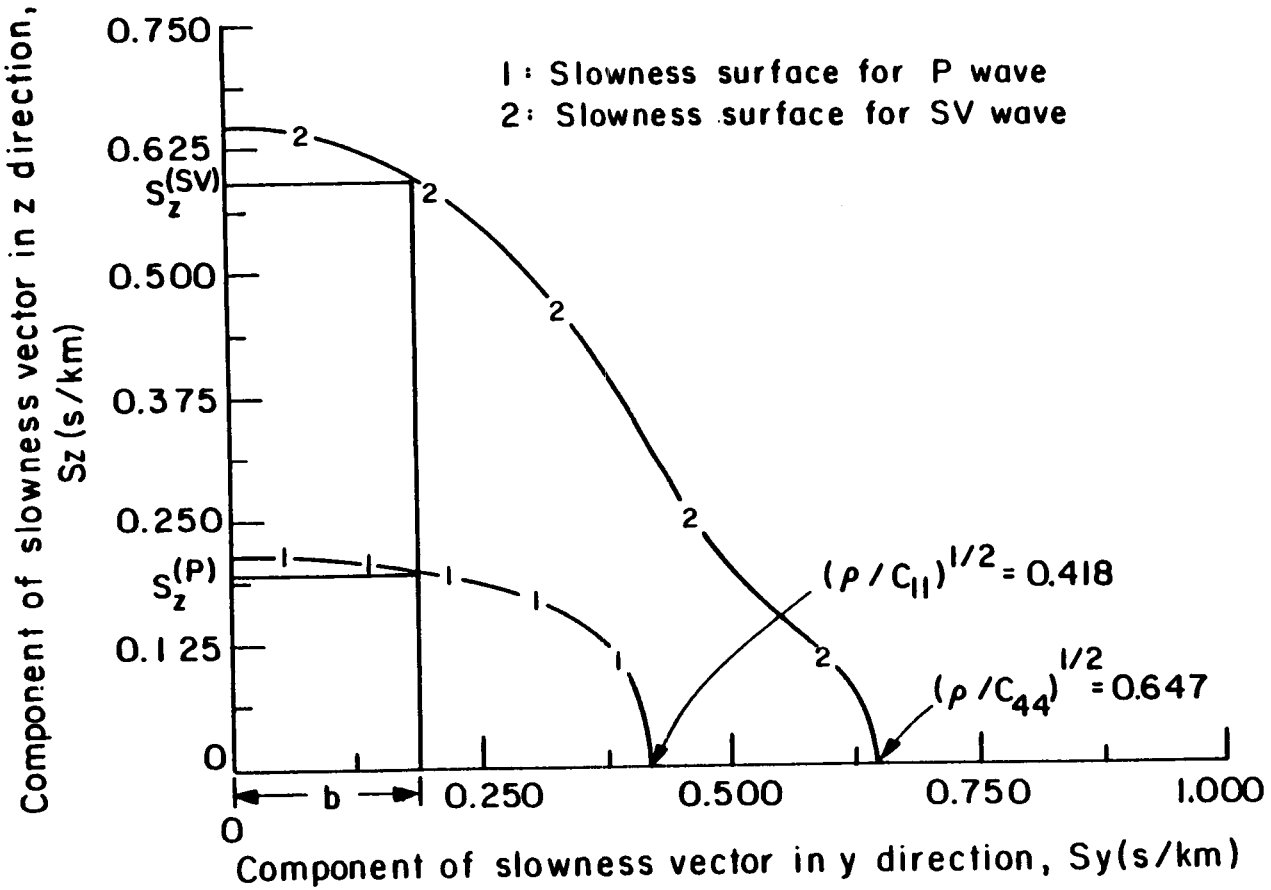

Fig. 3 Two sheets of slowness surface for P and SV waves in unidirectional fiberglass epoxy composite for positive y-z quadrant.

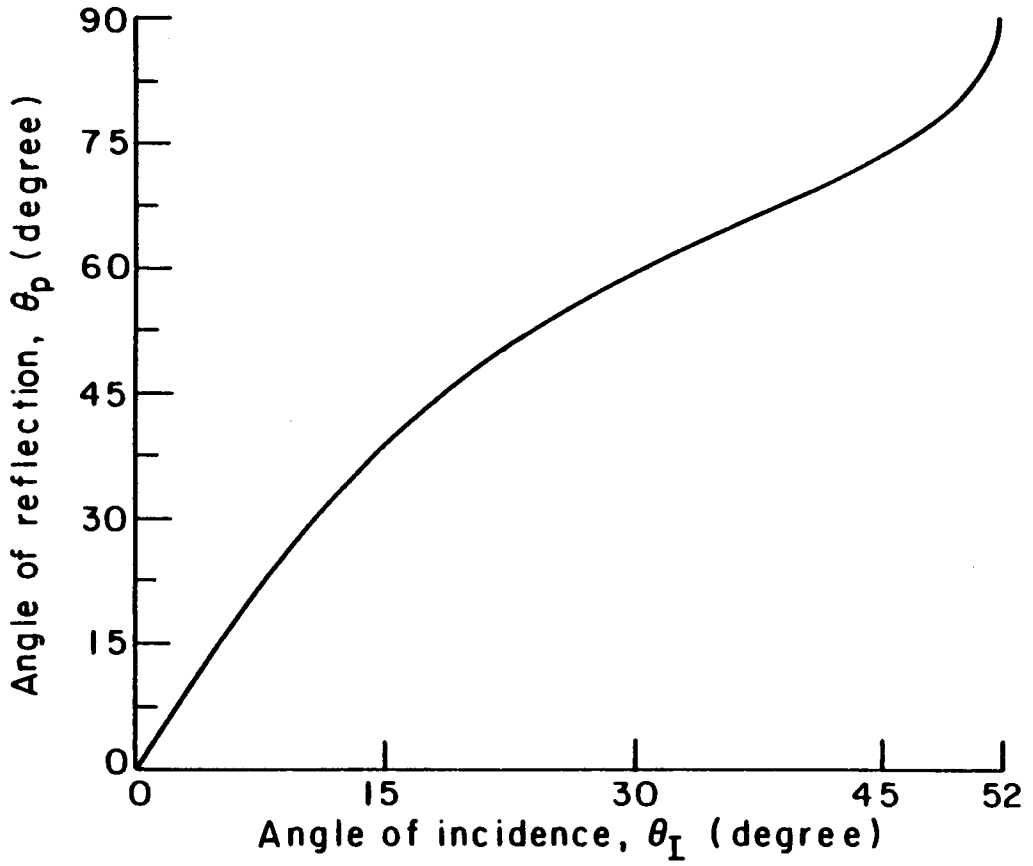

Fig. 4 Angle of reflection of reflected P wave versus angle of incidence of incident SV wave in unidirectional fiberglass epoxy composite.

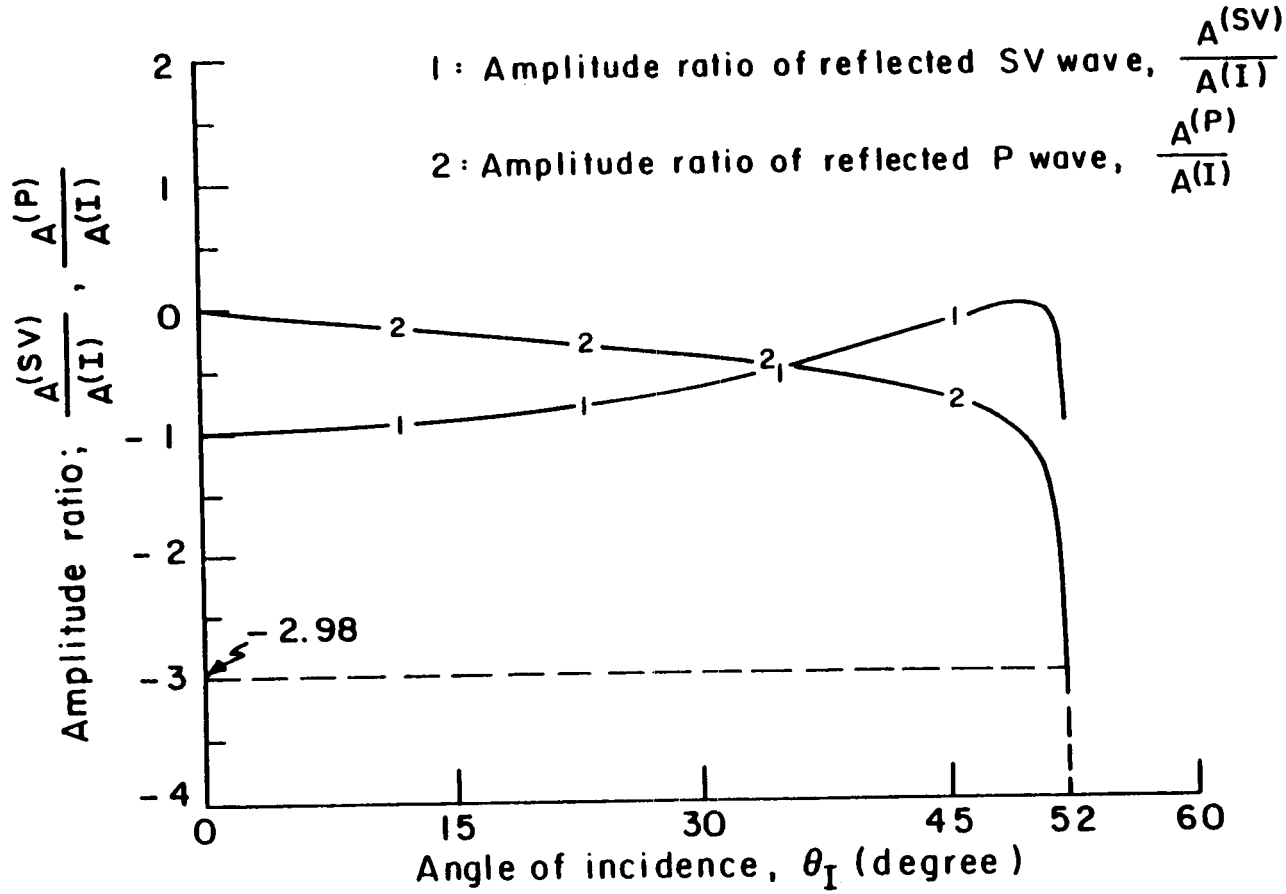

Fig. 5 Amplitude ratios of reflected SV and P waves to incident SV wave versus angle of incidence in unidirectional fiberglass epoxy composite for angle of incidence less than critical angle.

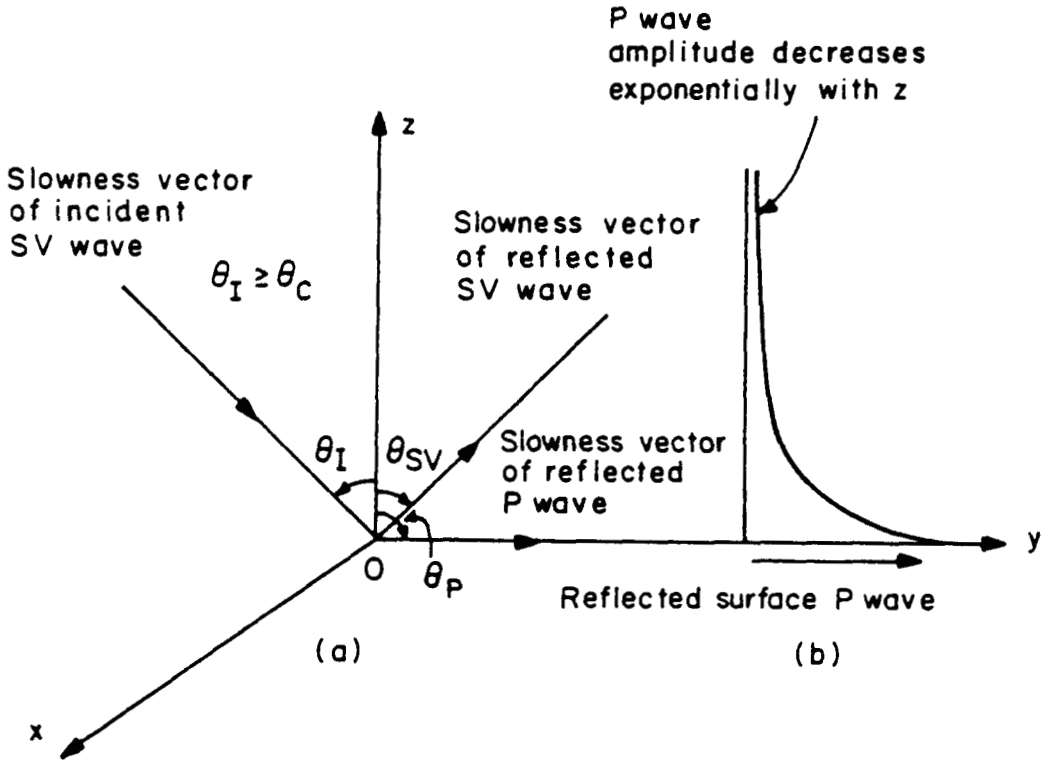

Fig. 6 Existence of reflected surface P wave whose amplitude decreases exponentially with z for angle of incidence of incident SV wave in unidirectional fiberglass epoxy composite, equal to or greater than critical angle θ_c; $z = 0$ is plane boundary where single reflection occurs, $z < 0$ is free space, and $x = 0$ is plane of incidence.

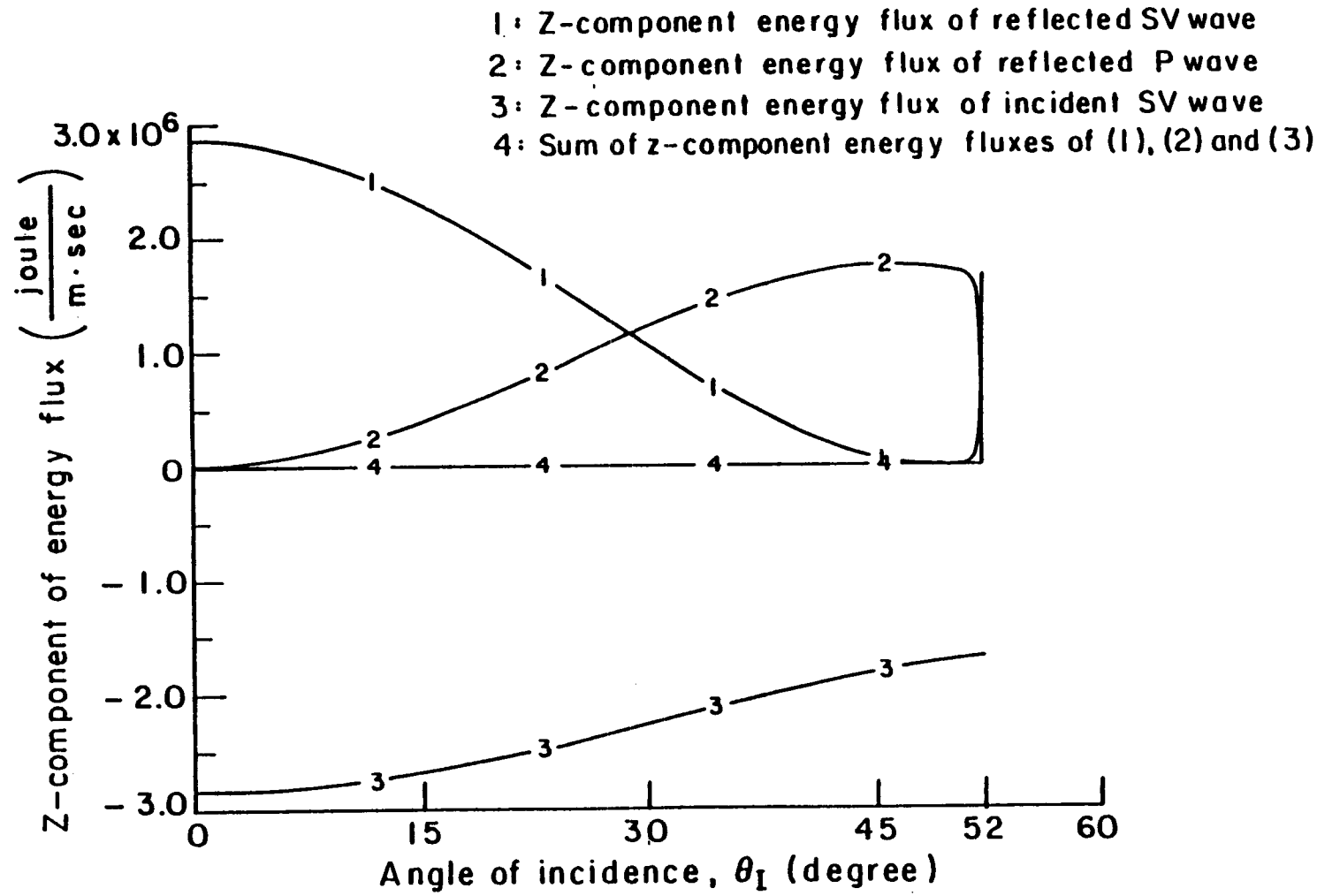

Fig. 7 Energy fluxes normal to plane boundary, assuming radian frequency equal to unity, for incident SV wave in unidirectional fiberglass epoxy composite for angle of incidence less than critical angle.

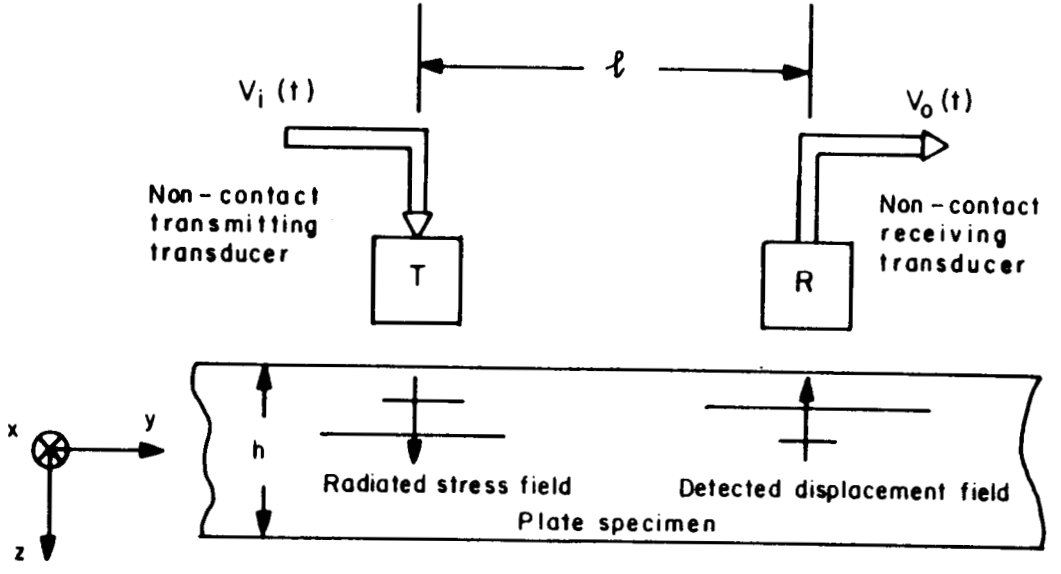

Fig. 8 Schematic of non-contact acousto-ultrasonic test configuration.

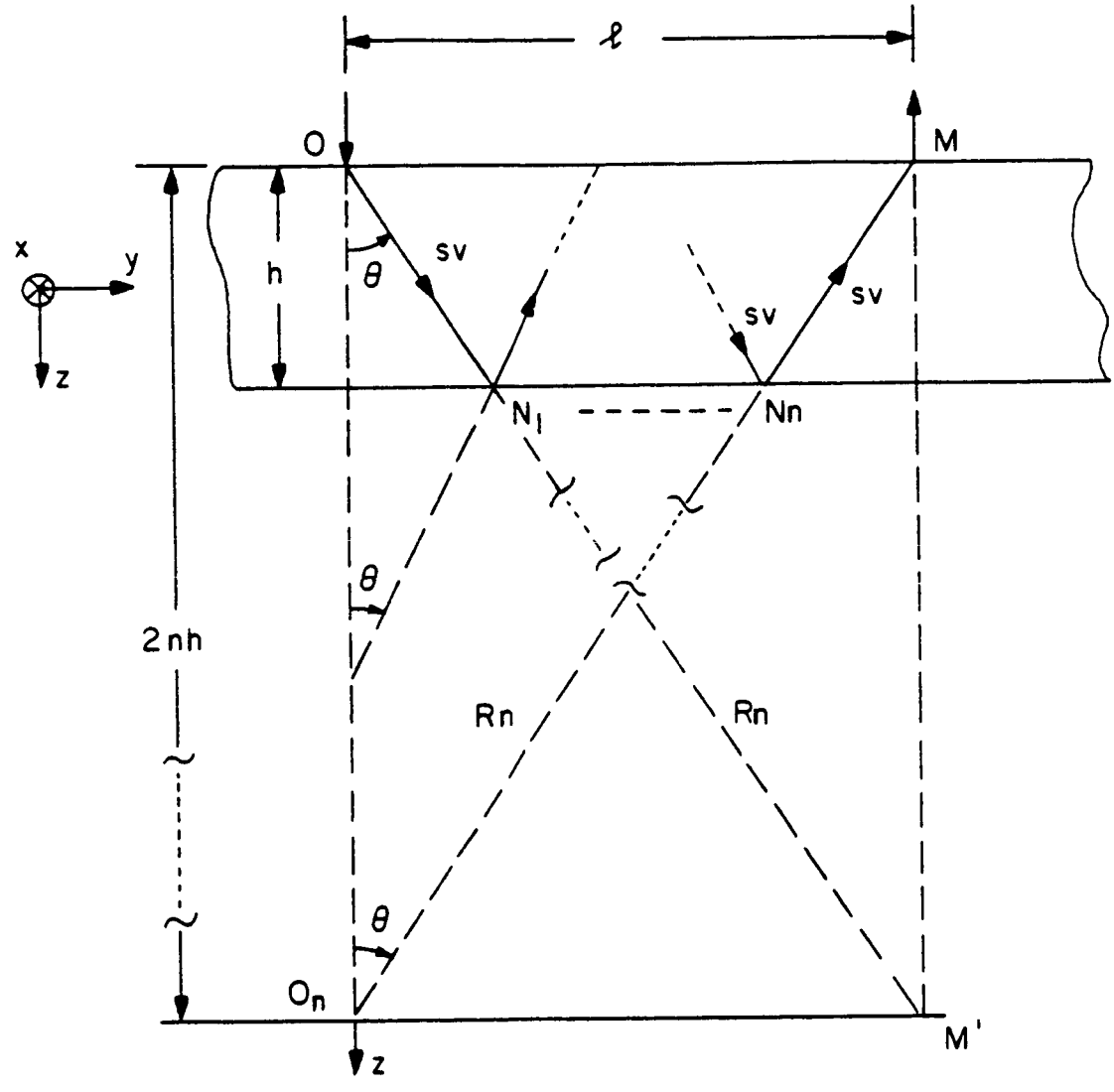

Fig. 9 Path of SV - SV - ... wave which arrives at point M after n reflections from bottom boundary.

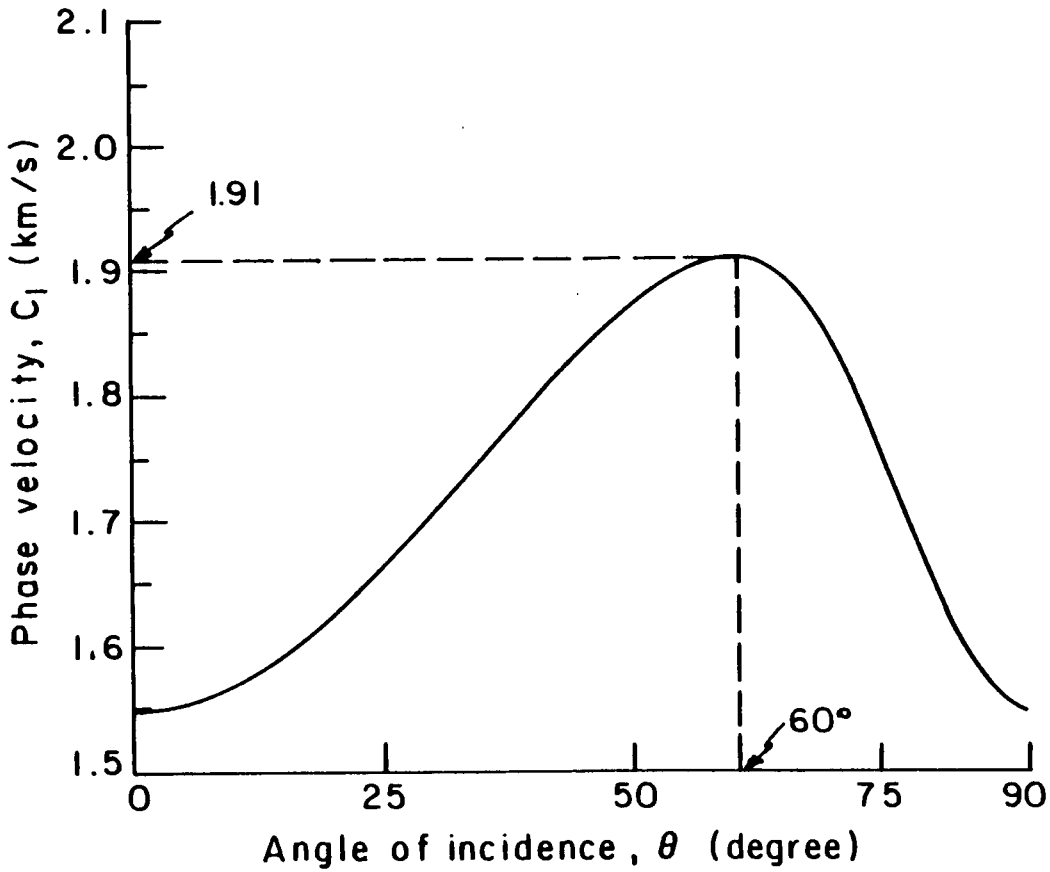

Fig. 10 Phase velocity versus angle of incidence for SV wave travelling in unidirectional fiberglass epoxy composite plate specimen.

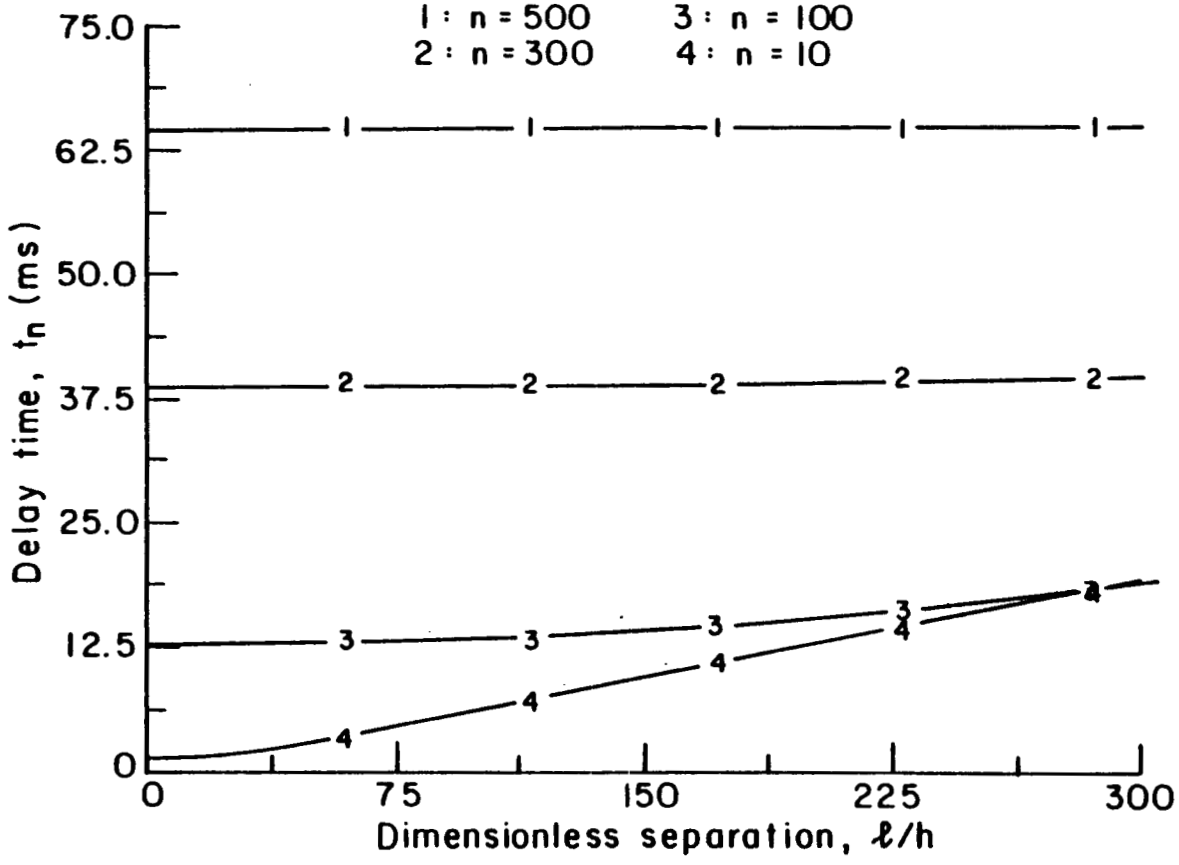

Fig. 11 Delay time versus dimensionless separation (ℓ/h) with number of reflections n from bottom face of unidirectional fiberglass epoxy composite plate specimen as parameter.

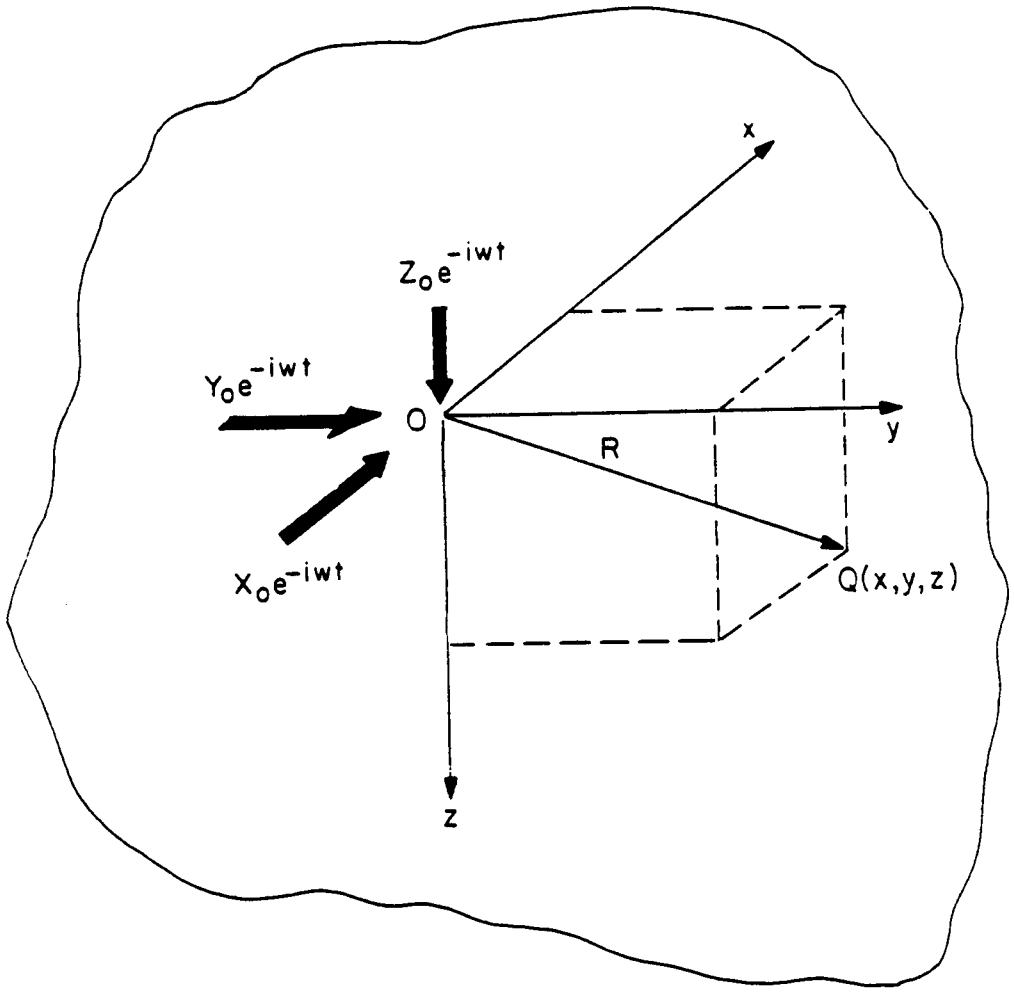

Fig. 12 Schematic illustrating sinusoidal point load exciting infinite transversely isotropic medium, where xy plane is isotropic plane in cartesian coordinate system defined by O(x,y,z).

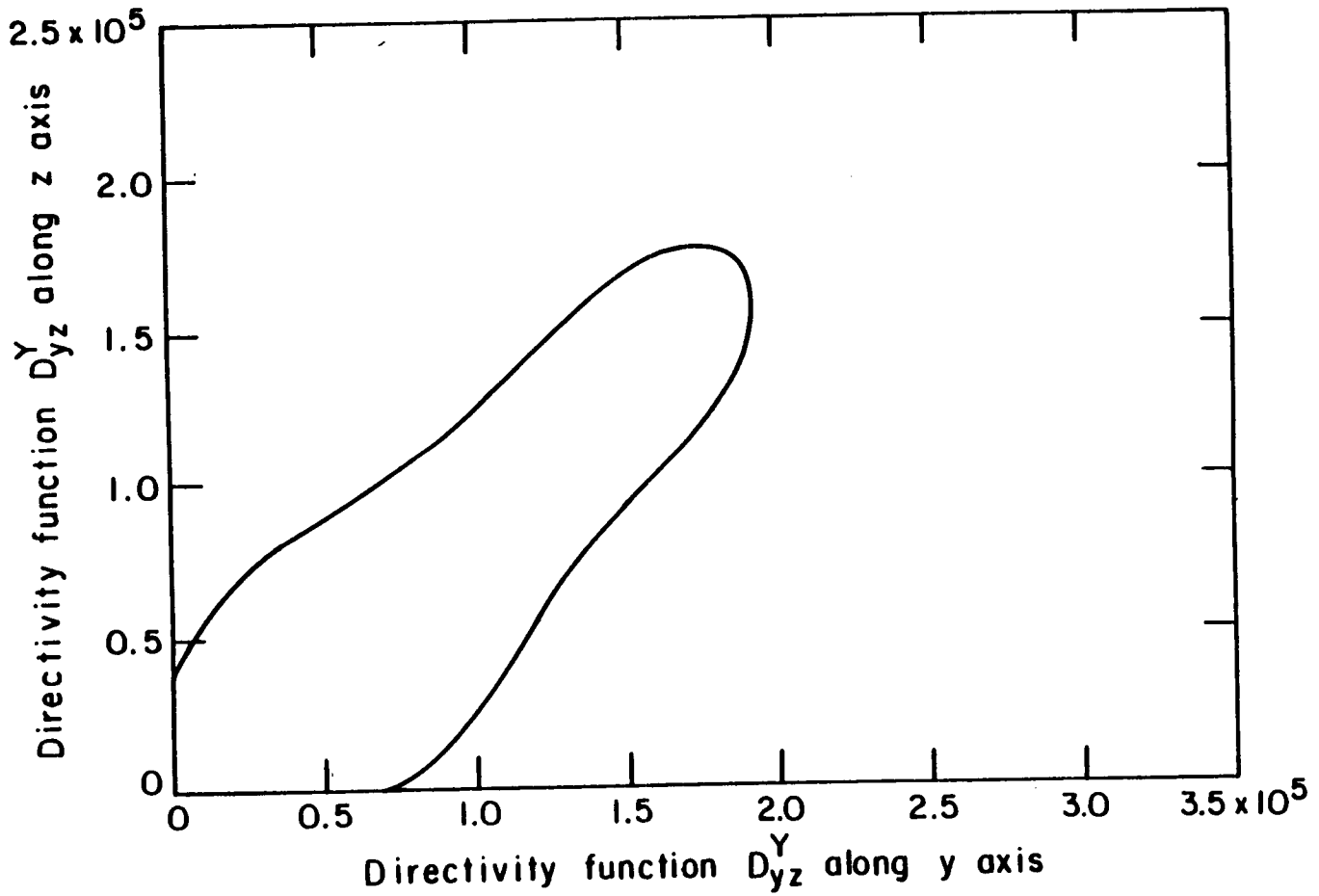

Fig. 13 Polar diagram for directivity function D^Y_{yz} of shear stress τ_{yz} at transmitting origin associated with SV wave in unidirectional fiberglass epoxy composite plate specimen at frequency of 0.75 MHz for positive y-z quadrant due to applied point force acting along y-direction.

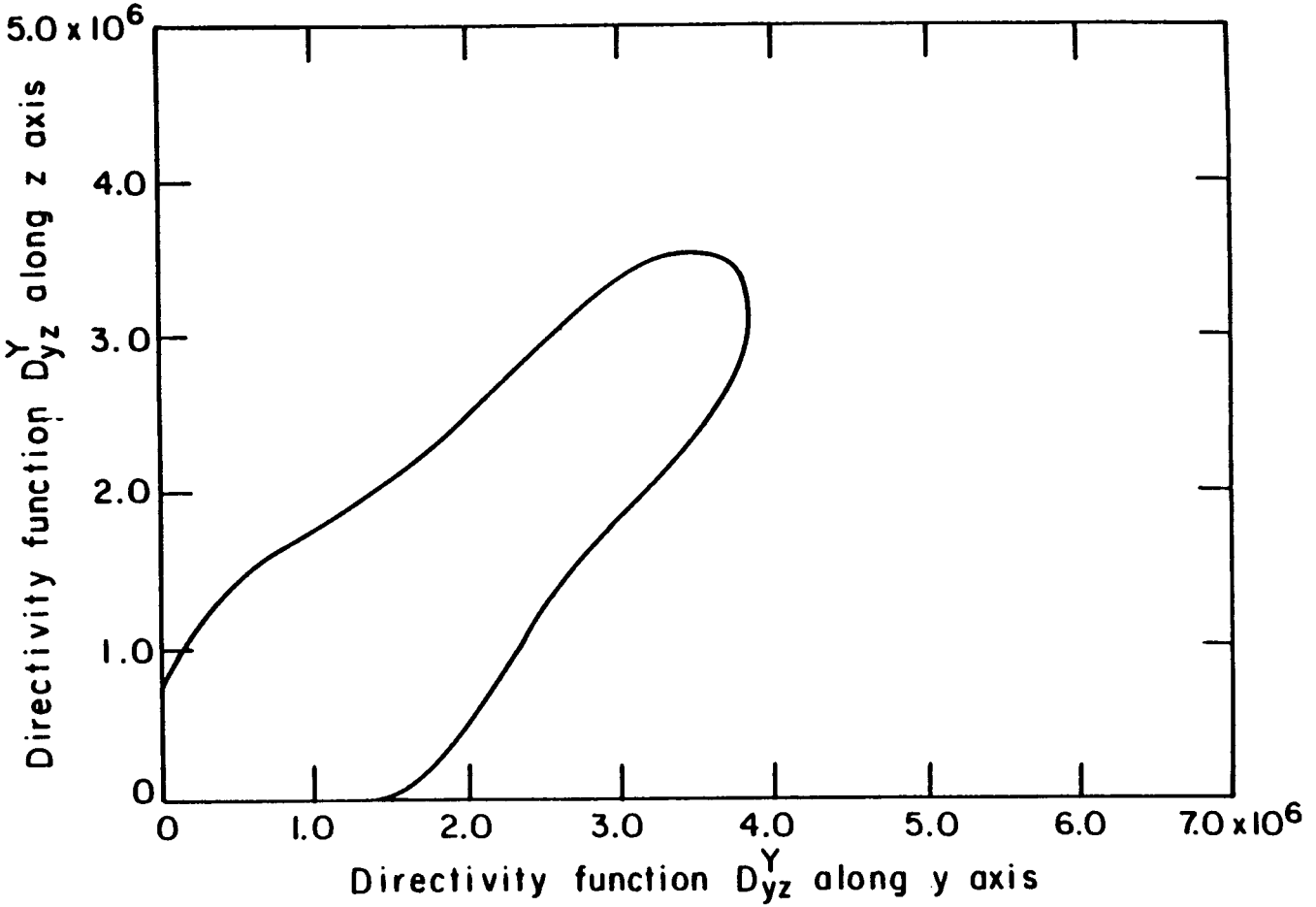

Fig. 14 Polar diagram for directivity function D_{yz}^{Y} of shear stress τ_{yz} at transmitting origin associated with SV wave in unidirectional fiberglass epoxy composite plate specimen at frequency of 1.50 MHz for positive y-z quadrant due to applied point force acting along y-direction.

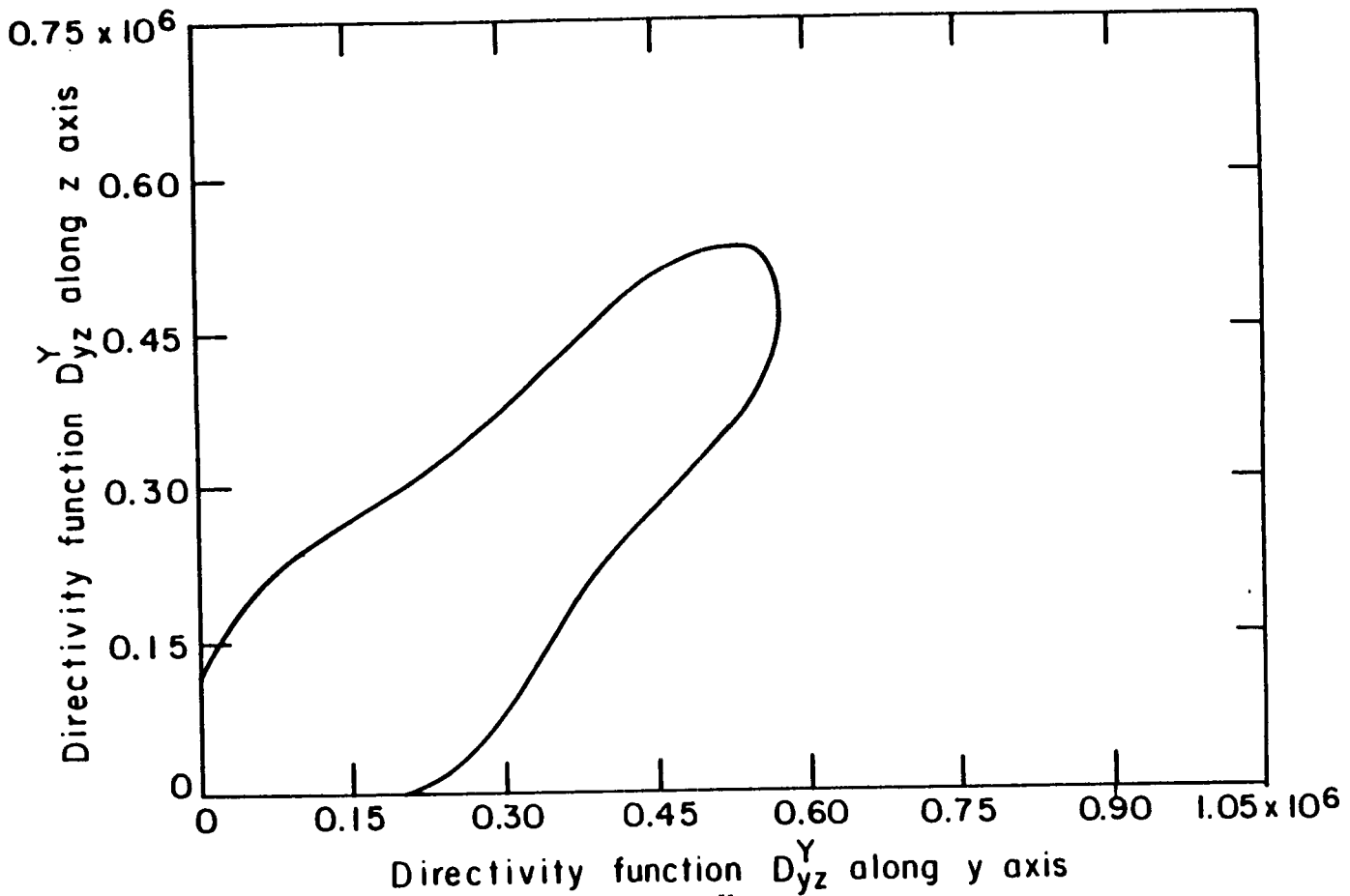

Fig. 15 Polar diagram for directivity function D_{yz}^{Y} of shear stress τ_{yz} at transmitting origin associated with SV wave in unidirectional fiberglass epoxy composite plate specimen at frequency of 2.25 MHz for positive y-z quadrant due to applied point force acting along y-direction.

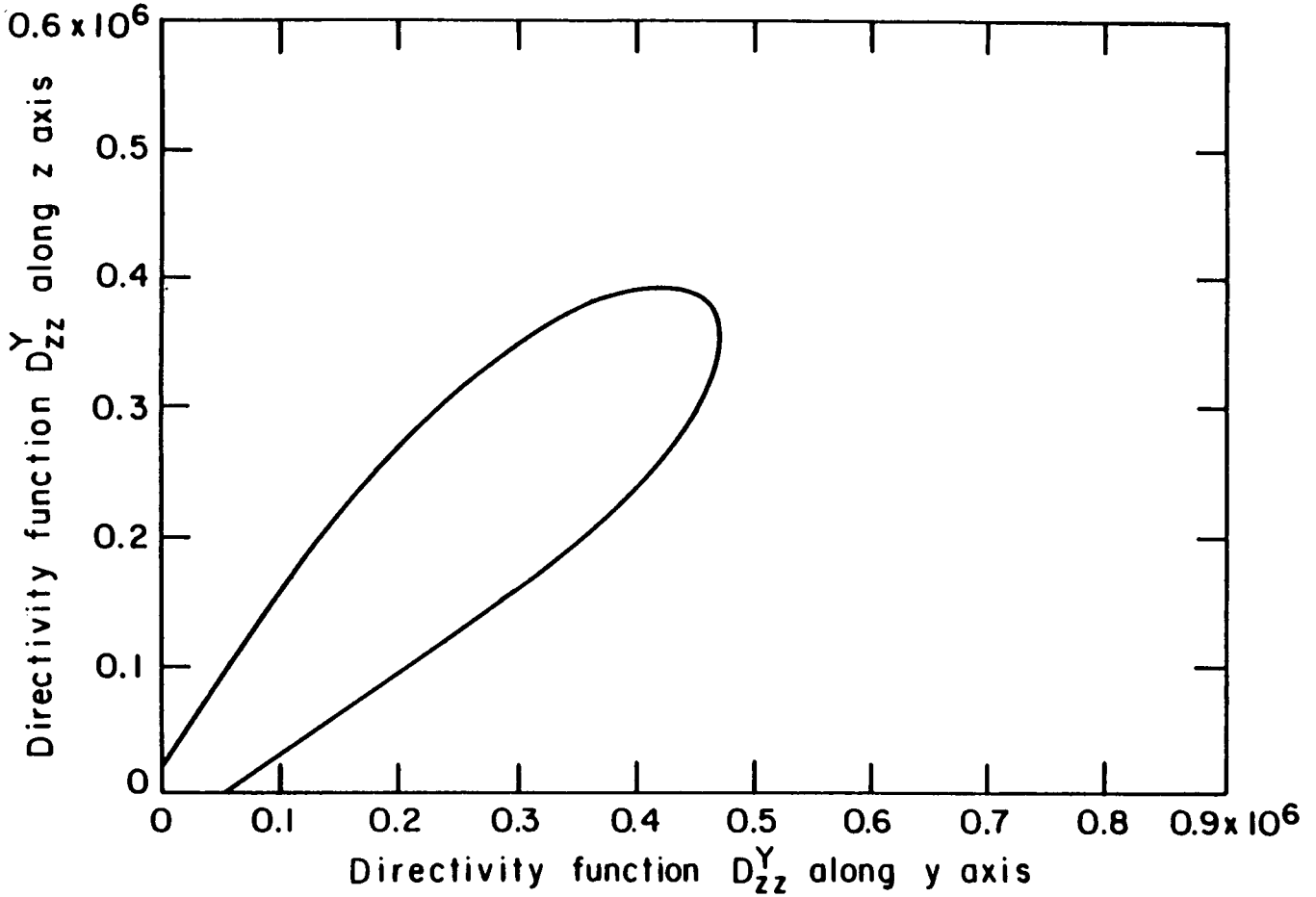

Fig. 16 Polar diagram for directivity function D^Y_{zz} of normal stress τ_{zz} at transmitting origin associated with SV wave in unidirectional fiberglass epoxy composite plate specimen at frequency of 0.75 MHz for positive y-z quadrant due to applied point force acting along y-direction.

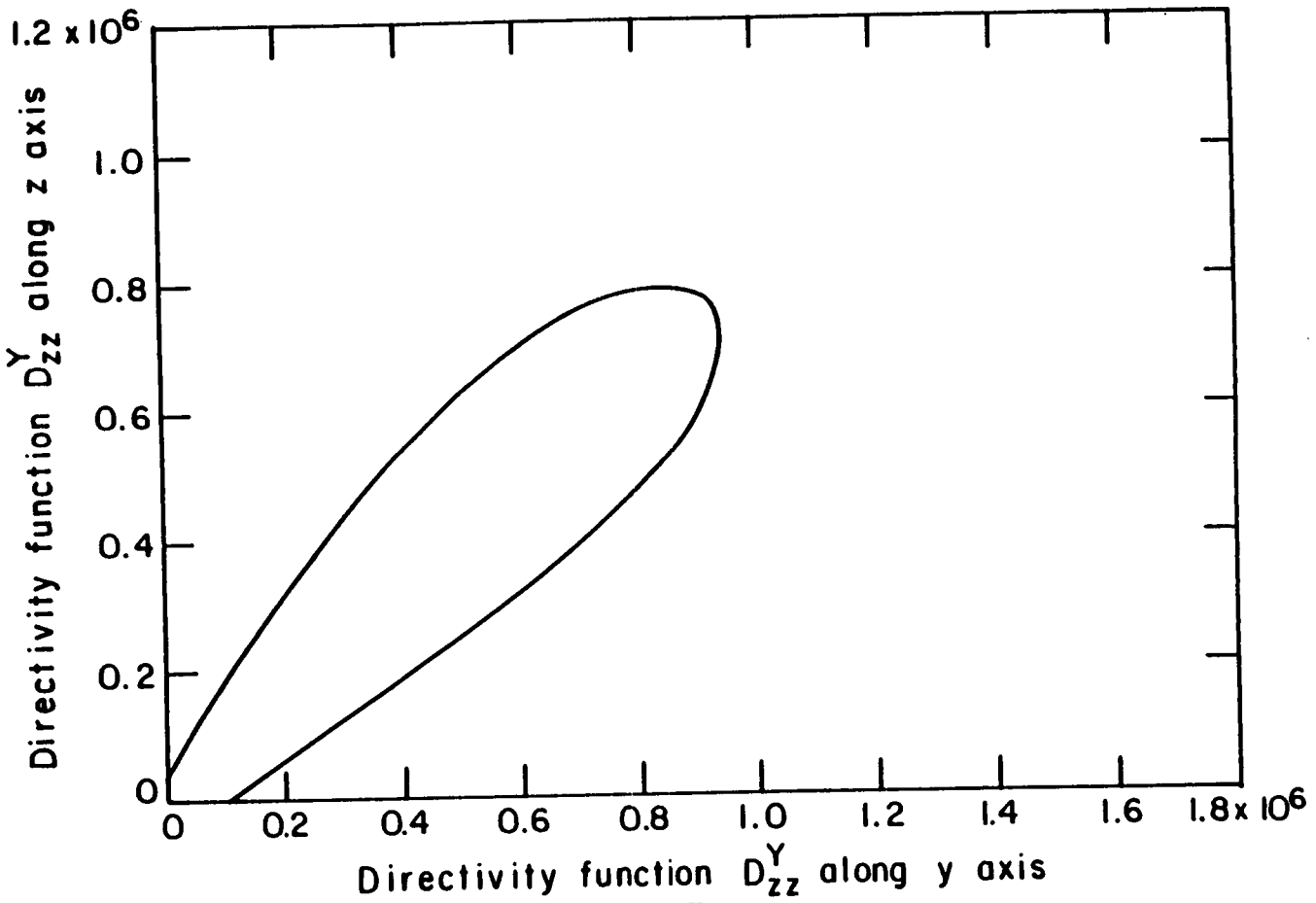

Fig. 17 Polar diagram for directivity function D_{zz}^{Y} of normal stress τ_{zz} at transmitting origin associated with SV wave in unidirectional fiberglass epoxy composite plate specimen at frequency of 1.50 MHz for positive y-z quadrant due to applied point force acting along y-direction.

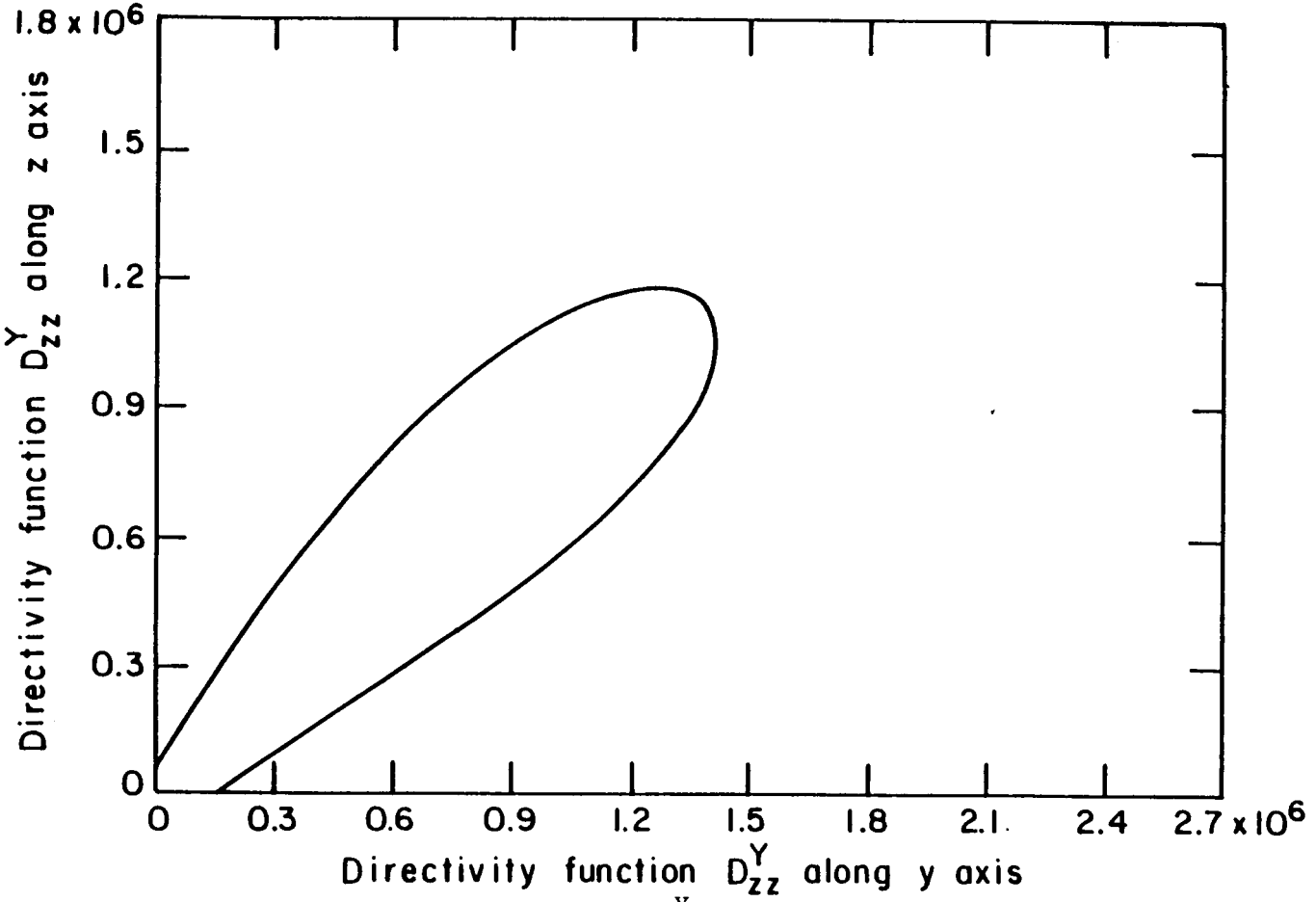

Fig. 18 Polar diagram for directivity function D_{zz}^{Y} of normal stress τ_{zz} at transmitting origin associated with SV in unidirectional fiberglass epoxy composite plate specimen at frequency of 2.25 MHz for positive y-z quadrant due to applied point force acting along y-direction.

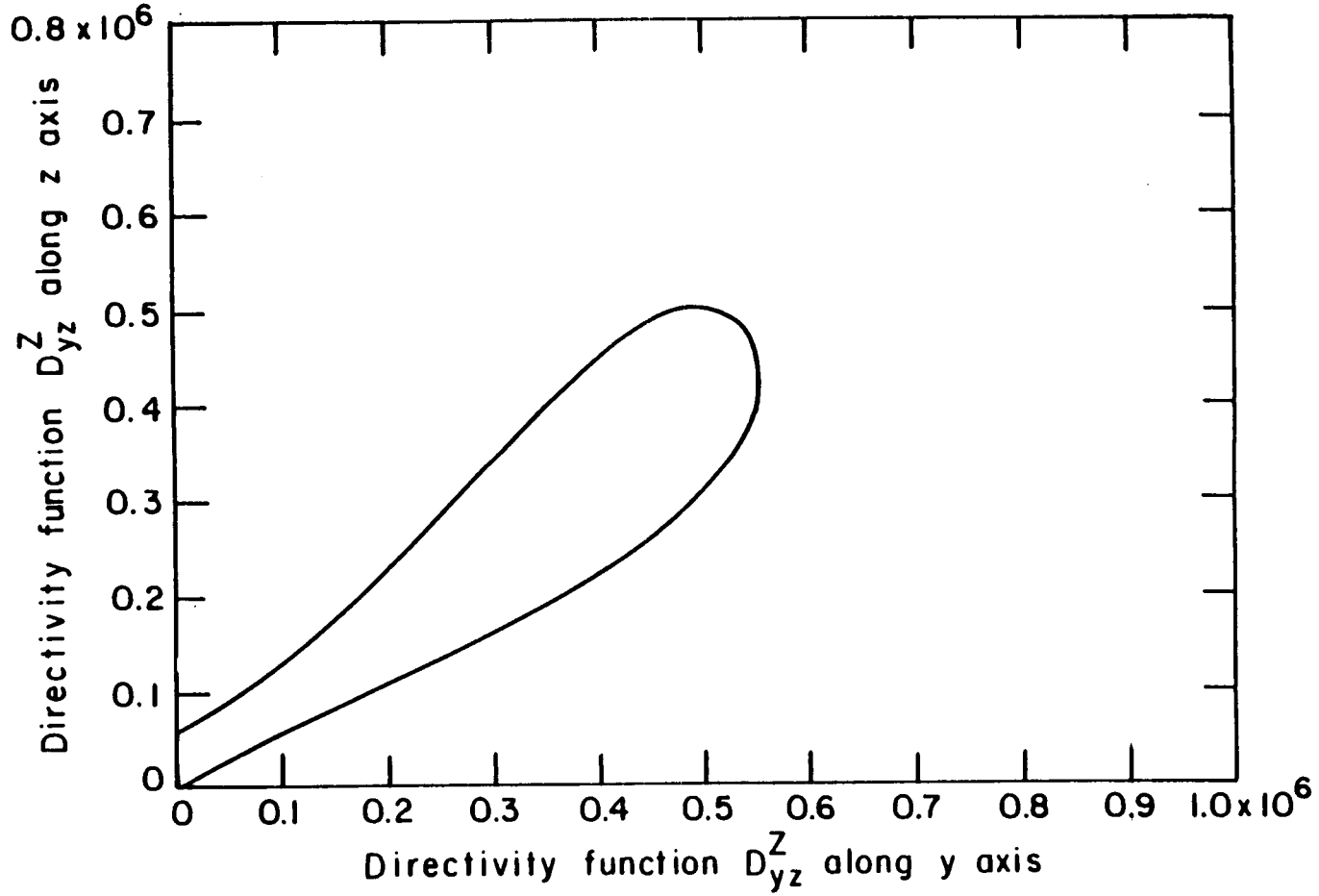

Fig. 19 Polar diagram for directivity function D_{yz}^{z} of shear stress τ_{yz} at transmitting origin associated with SV wave in unidirectional fiberglass epoxy composite plate specimen at frequency of 0.75 MHz for positive y-z quadrant due to applied point force acting along z-direction.

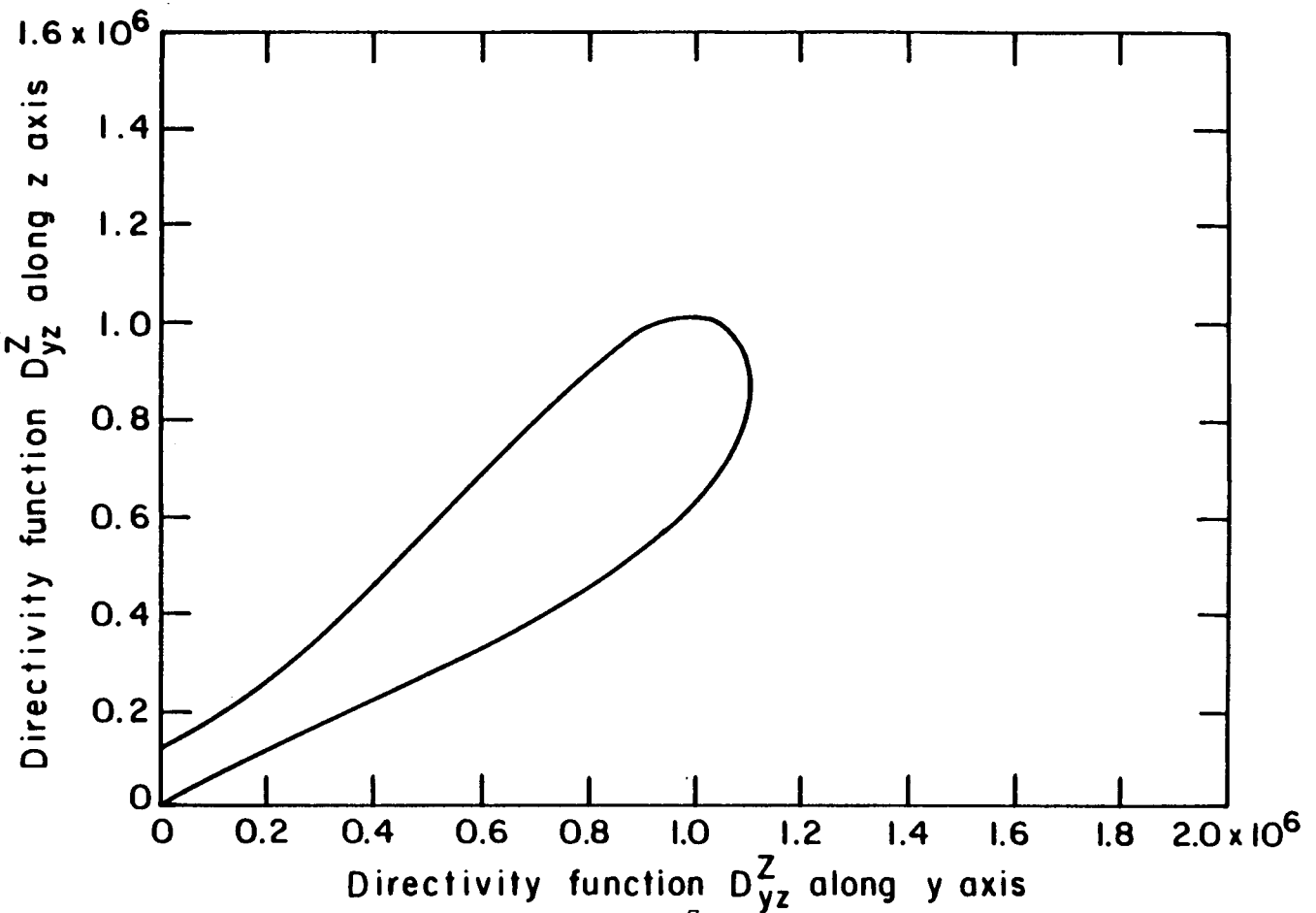

Fig. 20 Polar diagram for directivity function D_{yz}^{z} of shear stress τ_{yz} at transmitting origin associated with SV wave in unidirectional fiberglass epoxy composite plate specimen at frequency of 1.50 MHz for positive y-z quadrant due to applied point force acting along z-direction.

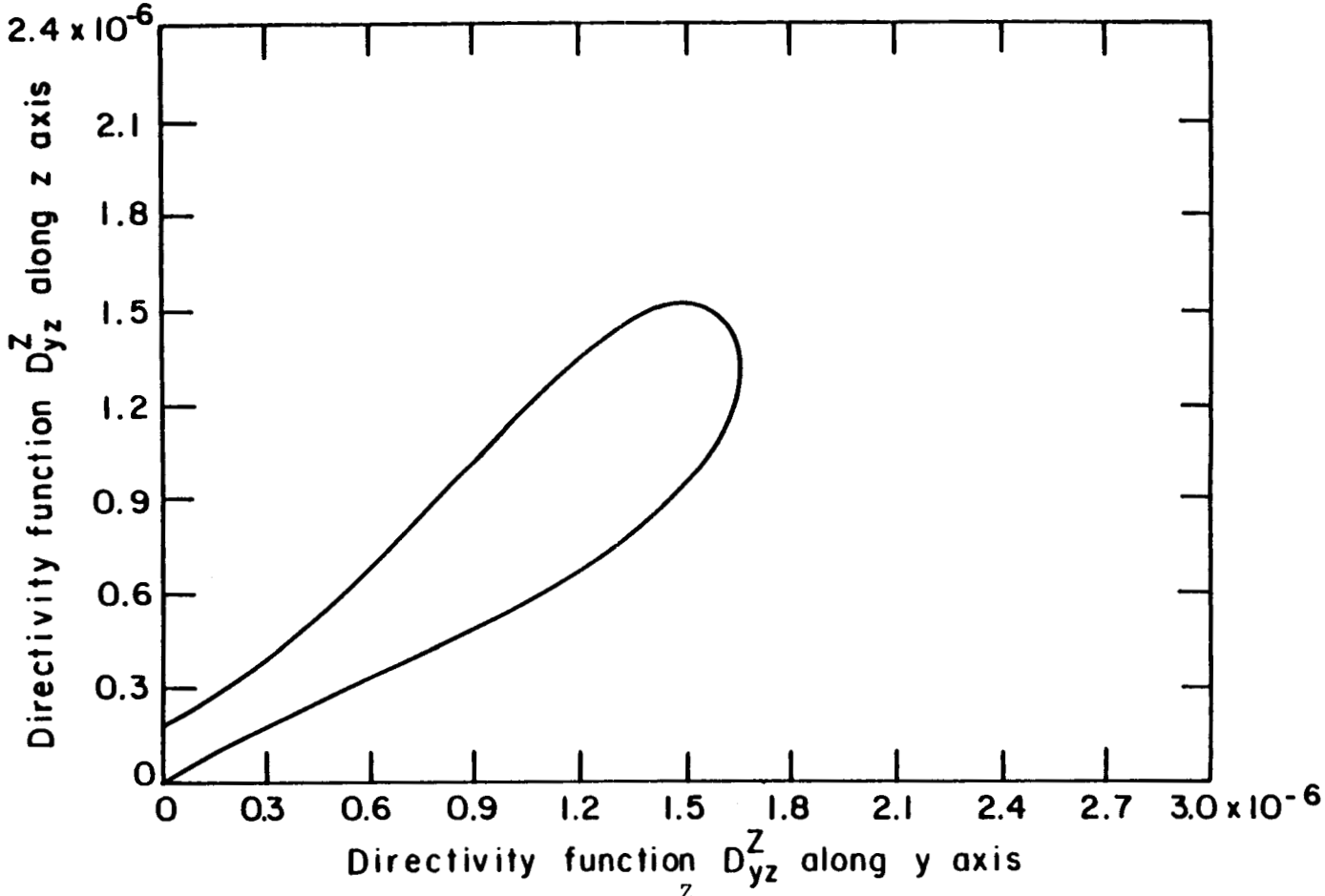

Fig. 21 Polar diagram for directivity function D^{Z}_{yz} of shear stress τ_{yz} at transmitting origin associated with SV wave in unidirectional fiberglass epoxy composite plate specimen at frequency of 2.25 MHz for positive y-z quadrant due to applied point force acting along z-direction.

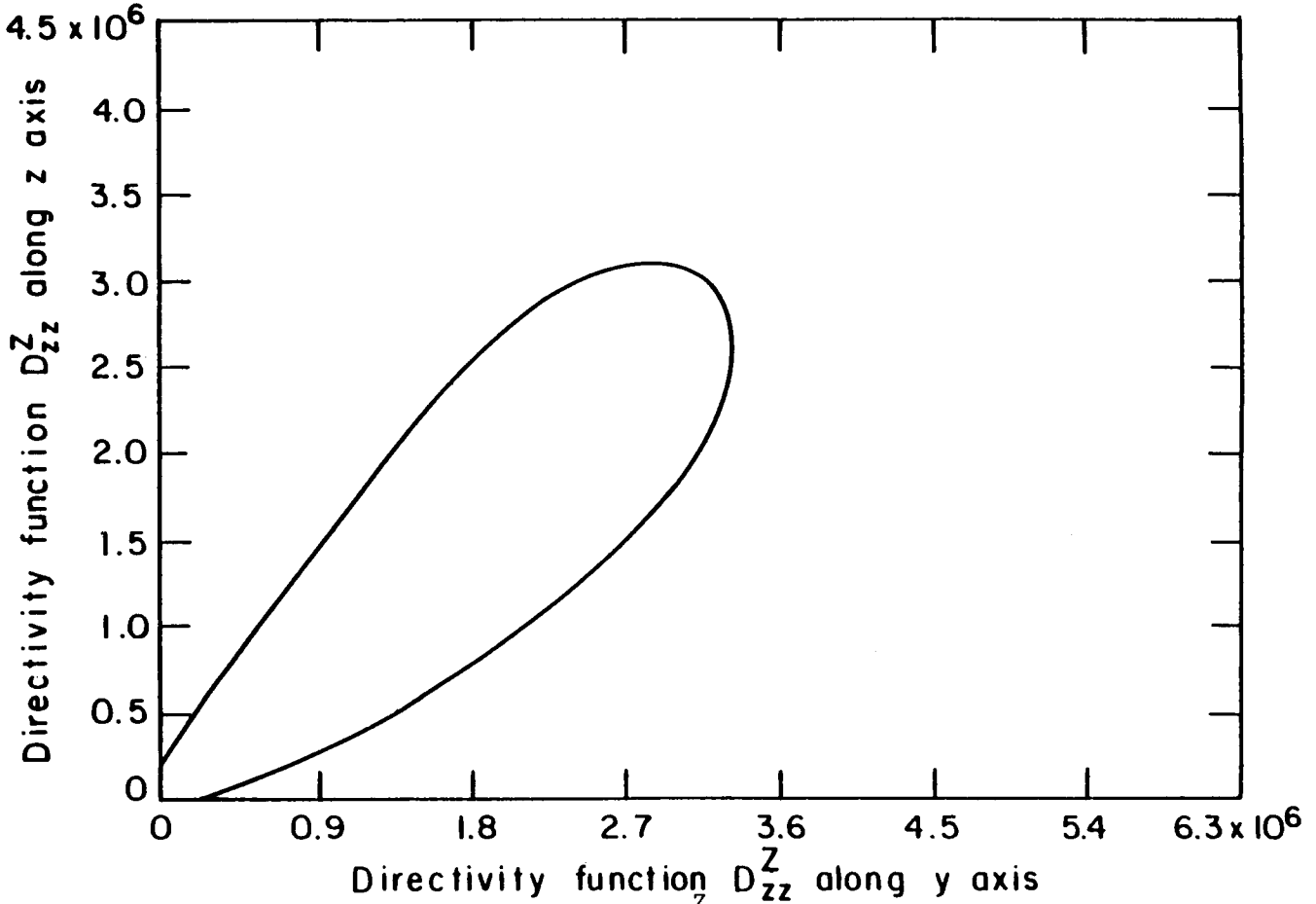

Fig. 22 Polar diagram for directivity function D_{zz}^{z} of normal stress τ_{zz} at transmitting origin associated with SV wave in unidirectional fiberglass epoxy composite plate specimen at frequency of 0.75 MHz for positive y-z quadrant due to applied point force acting along z-direction.

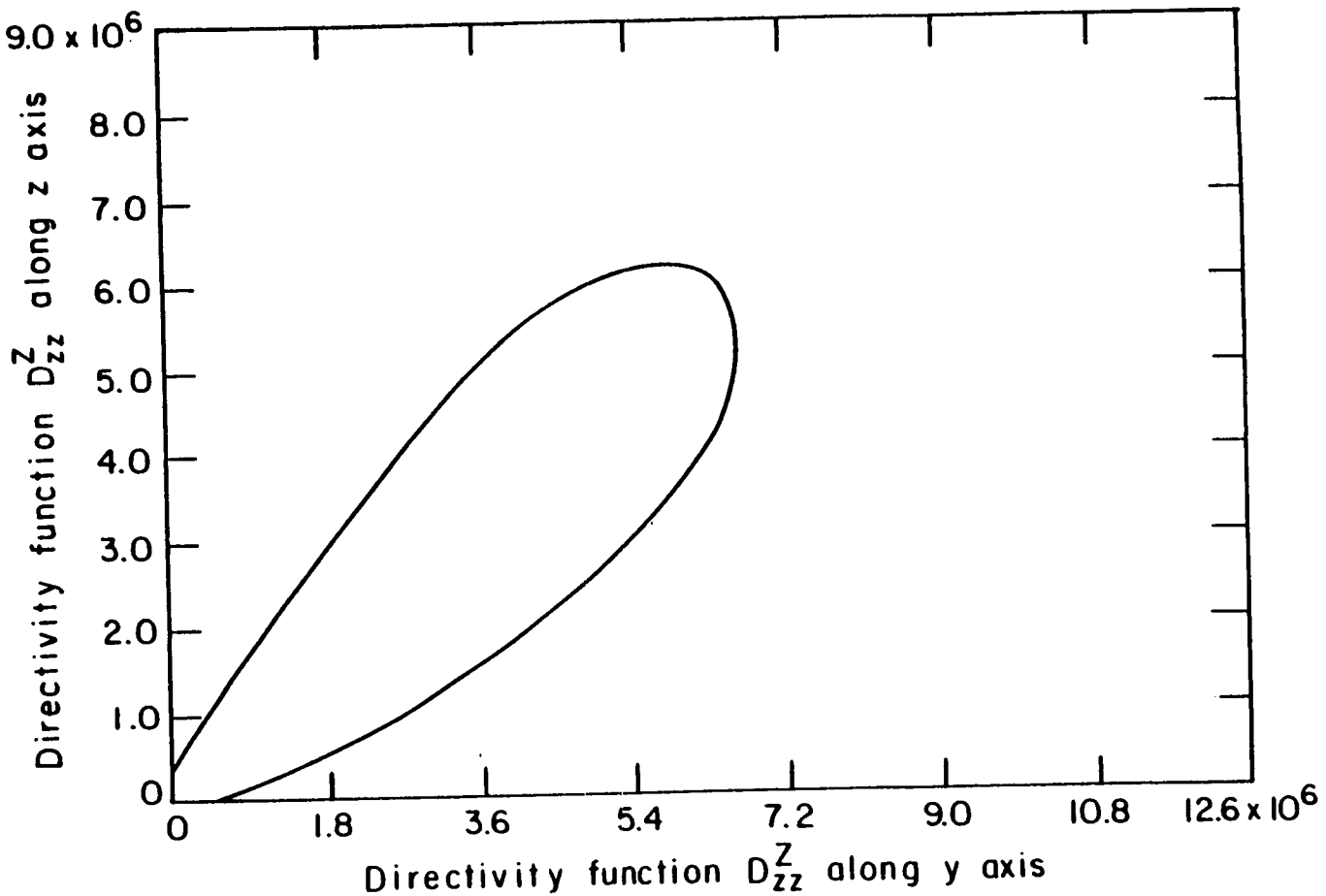

Fig. 23 Polar diagram for directivity function D_{zz}^{z} of normal stress τ_{zz} at transmitting origin associated with SV wave in unidirectional fiberglass epoxy composite plate specimen at frequency of 1.50 MHz for positive y-z quadrant due to applied point force acting along z-direction.

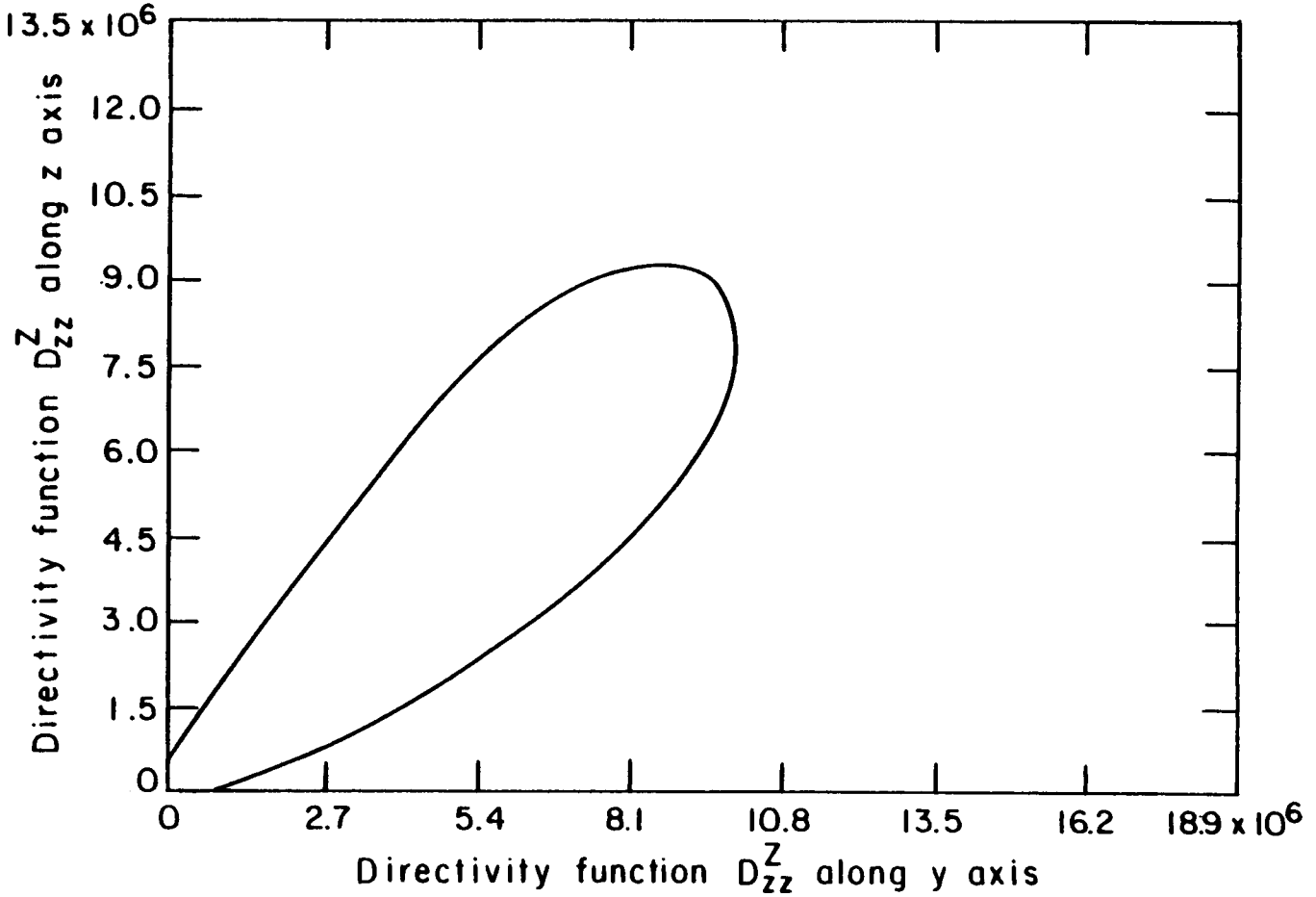

Fig. 24 Polar diagram for directivity function D^{Z}_{zz} of normal stress τ_{zz} at transmitting origin associated with SV wave in unidirectional fiberglass epoxy composite plate specimen at frequency of 2.25 MHz for positive y-z quadrant due to applied point force acting along z-direction.

NASA
National Aeronautics and Space Administration

Report Documentation Page

1. Report No.	2. Government Accession No.	3. Recipient's Catalog No.
NASA CR-4152		

4. Title and Subtitle
Acousto-Ultrasonic Input-Output Characterization of Unidirectional Fiber Composite Plate by SV Waves

5. Report Date
June 1988

6. Performing Organization Code

7. Author(s)
Peter Liao and James H. Williams, Jr.

8. Performing Organization Report No.
None (E-3996)

10. Work Unit No.
506-43-11

9. Performing Organization Name and Address
Massachusetts Institute of Technology
Dept. of Mechanical Engineering
Cambridge, Massachusetts 02139

11. Contract or Grant No.
NAG3-328

13. Type of Report and Period Covered
Contractor Report
Final

12. Sponsoring Agency Name and Address
National Aeronautics and Space Administration
Lewis Research Center
Cleveland, Ohio 44135-3191

14. Sponsoring Agency Code

15. Supplementary Notes
Project Manager, Harold E. Kautz, Structures Division, NASA Lewis Research Center.

16. Abstract
This study increases the quantitative understanding of acousto-ultrasonic nondestructive evaluation (NDE) parameters such as the stress wave factor (SWF) and wave propagation in fiber reinforced polymeric, ceramic or metallic composites, which can be modelled as transversely isotropic media. A unidirectional fiberglass epoxy composite specimen is modelled as a homogeneous transversely isotropic continuum plate medium. Acousto-ultrasonic noncontact input-output characterization is studied theoretically with a transmitting and a receiving transducer located on the same face of the plate. The single reflection problem for an incident SV wave at a plane boundary in transversely isotropic medium is analyzed. It is found that an obliquely incident SV wave results in a reflected SV wave and a reflected P wave for an angle of incidence of the incident SV wave less than the critical angle. When the angle of incidence of an incident SV wave is equal to or greater than the critical angle, there exists only an SV wave in the medium as the reflected P wave degenerates into a surface wave travelling parallel to the plane boundary. The amplitude ratio of the reflected SV wave is found to be minus one when the angle of incidence is equal to or greater than the critical angle. It is found that the directional dependence of the phase velocity of the SV wave propagating in the transversely isotropic medium has a significant effect on the delay time, as opposed to the directional independence of the phase velocity of a shear wave propagating in an isotropic medium. The displacements associated with the SV wave in the plate and which may be detected by the noncontact receiving transducer are approximated by an asymptotic solution for an infinite transversely isotropic medium subjected to a harmonic point load.

17. Key Words (Suggested by Author(s))
Nondestructive testing; Nondestructive evaluation; Ultrasonics; Acousto-ultrasonics; Stress wave factor; Wave analysis; Plate waves; Guided waves; Fiber reinforced composites

18. Distribution Statement
Unclassified - Unlimited
Subject Category 38

19. Security Classif. (of this report)	20. Security Classif. (of this page)	21. No of pages	22. Price*
Unclassified	Unclassified	89	A05

NASA FORM 1626 OCT 86

*For sale by the National Technical Information Service, Springfield, Virginia 22161 - NASA-Langley, 1988